A HYBRID-STRESS NONUNIFORM TIMOSHENKO BEAM FINITE ELEMENT

A THESIS SUBMITTED TO
THE GRADUATE SCHOOL OF NATURAL AND APPLIED SCIENCES
OF
MIDDLE EAST TECHNICAL UNIVERSITY

BY

UMUT DEMİRHİSAR

IN PARTIAL FULFILLMENT OF THE REQUIREMENTS
FOR
THE DEGREE OF MASTER OF SCIENCE
IN
MECHANICAL ENGINEERING

NOVEMBER 2007

Approval of the thesis:

A HYBRID-STRESS NONUNIFORM TIMOSHENKO BEAM FINITE ELEMENT

submitted by **UMUT DEMİRHİSAR** in partial fulfillment of the requirements for the degree of **Master of Science in Mechanical Engineering Department, Middle East Technical University** by,

Prof. Dr. Canan Özgen _____
Dean, Graduate School of Natural and Applied Sciences

Prof. Dr. Kemal İder _____
Head of Department, Mechanical Engineering

Prof. Dr. Süha Oral _____
Supervisor, Mechanical Engineering Dept., METU

Examining Committee Members:

Prof. Dr. Bülent Doyum _____
Mechanical Engineering Dept., METU

Prof. Dr. Süha Oral _____
Mechanical Engineering Dept., METU

Prof. Dr. Kemal İder _____
Mechanical Engineering Dept., METU

Prof. Dr. Haluk Darendeliler _____
Mechanical Engineering Dept., METU

Assoc. Prof. Uğur Polat _____
Civil Engineering Dept., METU

Date: _____

I hereby declare that all information in this document has been obtained and presented in accordance with academic rules and ethical conduct. I also declare that, as required by these rules and conduct, I have fully cited and referenced all material and results that are not original to this work.

Name, Last name: Umut Demirhisar

Signature:

ABSTRACT

A HYBRID-STRESS NONUNIFORM TIMOSHENKO BEAM FINITE ELEMENT

Demirhisar, Umut

M.S., Department of Mechanical Engineering

Supervisor : Prof. Dr. Süha Oral

November 2007, 70 pages

In this thesis, a hybrid-stress finite element is developed for nonuniform Timoshenko beams. The element stiffness matrix is obtained by assuming a stress field only. Since element boundaries are simply the element nodes, a displacement assumption is not necessary. Geometric and mass stiffness matrices are obtained via equilibrium and kinematics of deformation equations which are derived in the beam arbitrary cross-section. Utilizing this method eliminates the displacement assumption for the geometric and mass stiffness matrices. The element has six degrees of freedom at each node. Axial, flexural and torsional effects are considered. The torsional and distortional warping effects are omitted. Deformations due to shear is also taken into account.

Finally, some sample problems are solved with the element and results are compared with the solutions in the literature and commercial finite element programs (i.e. MSC/NASTRAN®).

Keywords: Finite Elemet Method, hybrid-stress, Timoshenko beam, buckling, vibration

ÖZ

HİBRİT-GERİLİM DEĞİŞKEN KESİTLİ TIMOSHENKO KİRİŞİ SONLU ELEMANI

Demirhisar, Umut
Yüksek Lisans, Makina Mühendisliği Bölümü
Tez Yöneticisi : Prof. Dr. Süha Oral

Kasım 2007, 70 sayfa

Bu tezde değişken kesitli Timoshenko kirişi için hibrit-gerilim sonlu elemanı geliştirilmiştir. Eleman direngenlik matrisi sadece gerilim alanı varsayımı yapılarak elde edilmiştir. Eleman sınırları basitçe eleman düğüm noktaları ile örtüştüğü için yer değiştirme varsayımı yapmaya gerek yoktur. Geometrik ve kütle direngenlik matrisleri kirişin herhangi bir kesitinden çıkarılan denge ve deformasyon kinematik denklemeleri kullanılarak elde edilmiştir. Bu metodun uygulanması, geometrik ve kütle direngenlik matrislerini elde ederken yer değiştirme varsayımı yapma ihtiyacını ortadan kaldırmaktadır. Elemanın her düğüm noktasında altı serbestlik derecesi vardır. Eksenel, bükme ve burulma etkileri dikkate alınırken burulma ve bozulma burkulma etkileri ihmal edilmiştir. Kesme etkilerinden kaynaklanan bozulmalar ise göz önüne alınmıştır.

Geliştirilen eleman kullanılarak bazı örnek problemler çözülmüş ve sonuçlar literatürden ve yaygın sonlu eleman çözücülerinden (MSC/NASTRAN® gibi) elde edilen sonuçlarla karşılaştırılmıştır.

Anahtar kelimeler: Sonlu Eleman Metodu, hibrit gerilim, Timoshenko kirişi, burkulma, titreşim

To my mother

ACKNOWLEDGMENTS

I would like to express my sincere appreciation to my supervisor Prof. Dr. Süha Oral for his guidance and support throughout this research effort. I consider myself fortunate to have had a mentor with the strong work ethic and unyielding patience of Prof. Dr. Süha Oral.

I would like to thank to Dr. Fatih Cıbır, Dr. Varlık Özerciyes, Dr. Tarkan Çalışkan, Özkan Murat and Nazım Akman for their technical and moral support. I also would like to thank to Dr. Muvaffak Hasan for his understanding and tolerance.

TABLE OF CONTENTS

LIST OF TABLES

LIST OF FIGURES

CHAPTER 1

INTRODUCTION

Nonuniform beams are used in many structural applications to achieve a better distribution of strength and weight and sometimes to satisfy architectural and functional requirements. In most of the engineering structures consisting of tapered beams, the width of the cross-section remains constant, while the height varies linearly or parabolicaly with length. The study deals with static, dynamic and stability analysis of linear elastic plane structures composed of beams with linearly variable height and constant width.

1.1 Objective and Scope of the Study

The objective of this study is to develop a hybrid stress nonuniform Timoshenko beam finite element with geometric and mass stiffness matrices.

During the course of work, axial, flexural and torsional effects are considered however the torsional and distorsional warping effects are omitted since the scope of the thesis does not covers the corresponding topics.

The variable section properties of nonuniform beam are defined with respect to beam length direction. Then a hybrid stress formulation is carried out to form element stiffness matrix by assuming a stress field to satisfy homogenous equilibrium equations.

The geometric and mass stiffness matrices are developed consistently via equilibrium and kinematics of deformation equations. This approach eliminates the necessity of displacement field assumption which is used in most of the finite element formulations for dynamic and stability analyses.

Before proceeding on the analysis of nonuniform Timoshenko beams, the element formulation is carried out for a simple case which is a uniform straight beam to ensure a level of confidence for finite element formulation of consistent mass and geometric stiffness matrices. The uniform element performance is cross-checked with solutions of elements obtained by anisoparametric interpolation approach.

In order to analyze nonuniform Timoshenko beams, a program is generated in the Fortran Power Station environment which solves the finite element formulation. By the use of the generated computer program, static, dynamic and stability analyses are performed. All the results are compared with the results in the literature or with conventional finite element program MSC/NASTRAN®.

1.2 Literature Survey

A detailed literature survey has been performed to get into structural analysis of both uniform and nonuniform beams. First hybrid stress finite element approach has been investigated to get basic knowledge about beam finite element applications. Then research has moved into nonuniform beam studies which have been carried out in the past.

There is continuing research on the development of elements that combine the accuracy of higher-order elements with the simple nodal configuration of lower order elements.

In 1981 an effective method has been introduced by Tessler and Dong [1] for Timoshenko beams. The methodology in which displacements and rotations are expressed by different order polynomials was later called “anisoparametric interpolation” by Tessler and Hughes [2].

However as the number of nodes is minimized, a deflection matching analysis becomes necessary to improve the stiffness of the element. In 1981 through this analysis a new shear correction factor that incorporates both the classical shear correction and the element properties are determined by Tessler and Hughes [3].

It is possible to formulate a two-node element in which the correct displacements and moments can be computed at any section of the element by the standard hybrid stress method [4] where only the boundary displacements are required. However, the derivation of the element mass and the geometric stiffness matrices requires a displacement assumption over the entire element.

In 1991 Oral [5] incorporated the anisoparametric displacement assumptions with a modified form of the hybrid stress functional to obtain the element – stiffness and consistent mass matrices for a two node Timoshenko beam element. A deflection matching analysis was not necessary and the use of classical shear correction was sufficient.

Non – uniform beams such as beams with cross-section varying along their lengths are used in many structural applications in an effort to achieve a better distribution of strength and weight. In 1943, Newmark developed an approximate method for determining static deflections and moments in beam structures consisting of uniform or nonuniform members [6].

In 1963, Lindberg constructed consistent mass and stiffness matrices for linearly tapered beam elements of rectangular, circular and triangular section utilizing a cubic displacement function [8].

A number of exact solutions to the elastic stability problem of simple nonuniform beams together with some tables and graphs can be found in Timoshenko and Gere [11].Stability analysis of frameworks with nonuniform members by the conventional finite element method was first done by Wang [12].

In 1970, Galagher and Lee introduced a general nonuniform beam element which can be considered as generalization of Linderberg's element by computing its flexural and geometric stiffness matrices on the basis of a cubic displacement function and were able to obtain very accurate results with just a few elements [9]..

In 1977, Just developed the exact stiffness matrices for linearly tapered beams of rectangular, box and I section [7].

In 1979, To gave explicit expressions for the element mass and stiffness matrices of linearly tapered beam finite element including shear deformation and rotary inertia. The element cross-section rotation was assumed to be a sum of the slope of the transverse displacement and shear [17].

In 1983, Rutledge and Beskos developed stiffness and consistent mass matrices for a linearly tapered beam of rectangular section and constant width which give results slightly better than those of Galagher and Lee [10].

In 1983, Karabalis and Beskos proposed a finite element methodology for static, free vibration and stability analyses of linear elastic plane structures consisting of tapered beams [13].The method was based on the development of flexural stiffness,

axial stiffness', geometric stiffness and consistent mass matrices for a beam element of constant width and linearly varying depth. The element flexural and axial stiffness matrices were derived on the basis of displacement functions which are the exact solutions of the governing equations. The element geometric stiffness matrix was constructed on the basis of shape functions corresponding to the exact static displacement function of the tapered element. The element consistent mass matrix was constructed on the basis of shape functions corresponding to the cubic displacement function of a uniform beam.

In 1985, Gupta derived stiffness and consistent mass matrices for linearly tapered beam element of any cross-sectional shape in explicit form. Exact expression for the required displacement functions were used in the derivation of matrices. Variation of area and moment of inertia of the cross section along the axis of the element is exactly represented by simple functions involving shape factors [18].

In 1988, Cleghorn and Tabarrok developed a finite element model for free vibration analysis of linearly tapered Timoshenko beams via obtaining the shape functions from the homogenous solutions of the governing equations for static deflections [19].

In 1991, Lee and Kuo gave the exact static deflection of a nonuniform Timoshenko beam with typical kinds of boundary condition in closed form and expressed the static deflection in terms of the four fundamental solutions of the governing differential equation [14].

In 1992 , Friedman and Kosmatka developed the exact bending stiffness matrix for an arbitrary non uniform beam including shear deformation based on Timoshenko beam theory [15].In the paper, numerical examples were presented to asses the

interaction of taper rate and shear deformation on the behavior of short beams.

In 1995, Romano presented closed form solutions for bending beams with linearly and parabolically varying depth and for bending beams with linearly varying width along the beams length by taking into account the shear deformation of the beam. The solutions were achieved by transforming the fourth order differential equations with variable coefficients into fourth order differential equations with constant coefficients [16].

In 1995, De Rosa and Franciosi used Timoshenko quotient for stability analysis of rectangular beams with linearly varying height. An iterative procedure was suggested which leads to closer approximations to the true results [20].

In 2004, Aucellio and Ercolano proposed a dynamic investigation method for the analysis of Timoshenko beams which takes into account the shear deformations and rotating inertia. The solution of the problem was obtained through the iterative variational Rayleigh – Ritz method and assuming as test functions an appropriate class of orthogonal polynomials which respect the essential conditions only [21].

CHAPTER 2

TIMOSHENKO BEAM THEORY

2.1 Kinematics of Deformation

The basic assumption in beam bending analysis excluding shear deformations is that a normal to the mid-surface (neutral axis) of the beam remains straight during deformation and that its angular rotation is equal to the slope of the beam mid-surface. This kinematic assumption corresponds to the Bernoulli beam theory.

Considering beam bending analysis with the effect of shear deformations, the assumption that a plane section originally normal to the neutral axis remains plane is retained, but because of shear deformations this section does not remain normal to the neutral axis. This kinematic assumption corresponds to Timoshenko beam theory.

XY Bending of a Symmetric Timoshenko Beam:

Consider beam deformations in two steps. In the first step consider bending only. AB & CD will remain normal to each other and go through a rotation $\psi_{(x)}$.

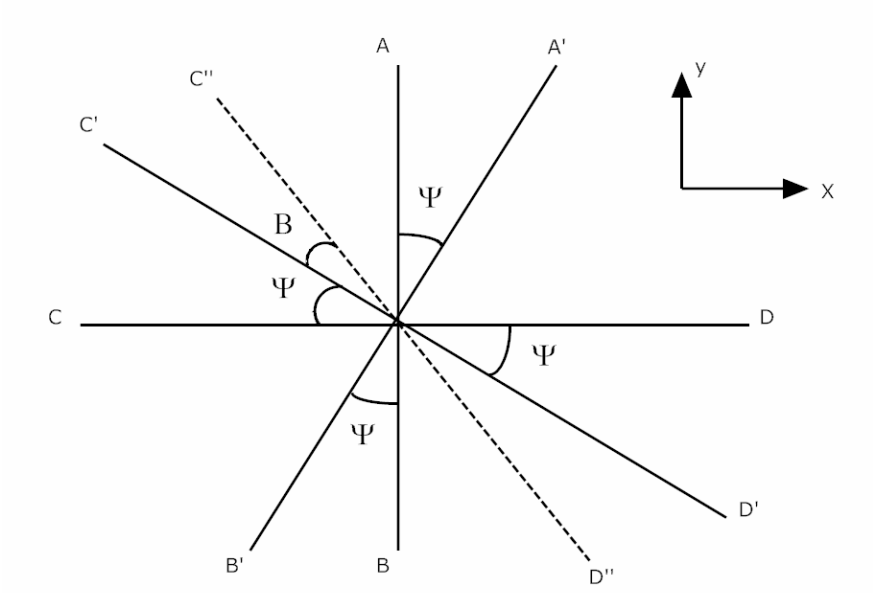

Figure – 2.1 Deformed and undeformed shape of a symmetric beam in xy plane

For the deformation,

$$\begin{aligned} u(x,y,z) &= -y\psi(x) \\ v(x,y,z) &= v(x) \\ w(x,y,z) &= 0 \end{aligned} \tag{2.1}$$

$$\begin{aligned} \sigma_{xy} &= 2G\varepsilon_{xy} = 0 \\ \sigma_{yz} &= 2G\varepsilon_{yz} = G\left(v_{,x} - \psi\right) \\ \sigma_{xz} &= 2G\varepsilon_{xz} = 0 \end{aligned} \tag{2.2}$$

σ_{zz} is almost zero since there is no loading on the sides of the beam. Furthermore σ_{yy} can be assumed to be negligible with respect to σ_{xx} because there is zero surface load on the bottom surface.

Then,

$$\sigma_{xx} = 2E\varepsilon_{xx} = -Ez\psi_{,x}$$
$$\sigma_{yy} = 0 \qquad (2.3)$$
$$\sigma_{zz} = 0$$

Shear stress at section x is free from the z direction by introducing a shear correction factor k.

$$\sigma_{yx} = kG\left(v_{,x} - \psi\right) \qquad (2.4)$$

By integrating the stresses over the cross-sectional area A to obtain the stress resultants,

$$Q_y = kGA\left(v_{,x} - \psi\right) \qquad (2.5)$$

$$M_y = -E\psi_{,x}\int y^2 dA \qquad (2.6)$$

$\int y^2 dA$ is the second moments of inertia on y axis: I_{zz}.

Then equation 2.6 can be written as,

$$M_z = -EI_{zz}\psi_{,x} \qquad (2.7)$$

Figure 2.2 shows deformations in 3D space for a Timoshenko beam.

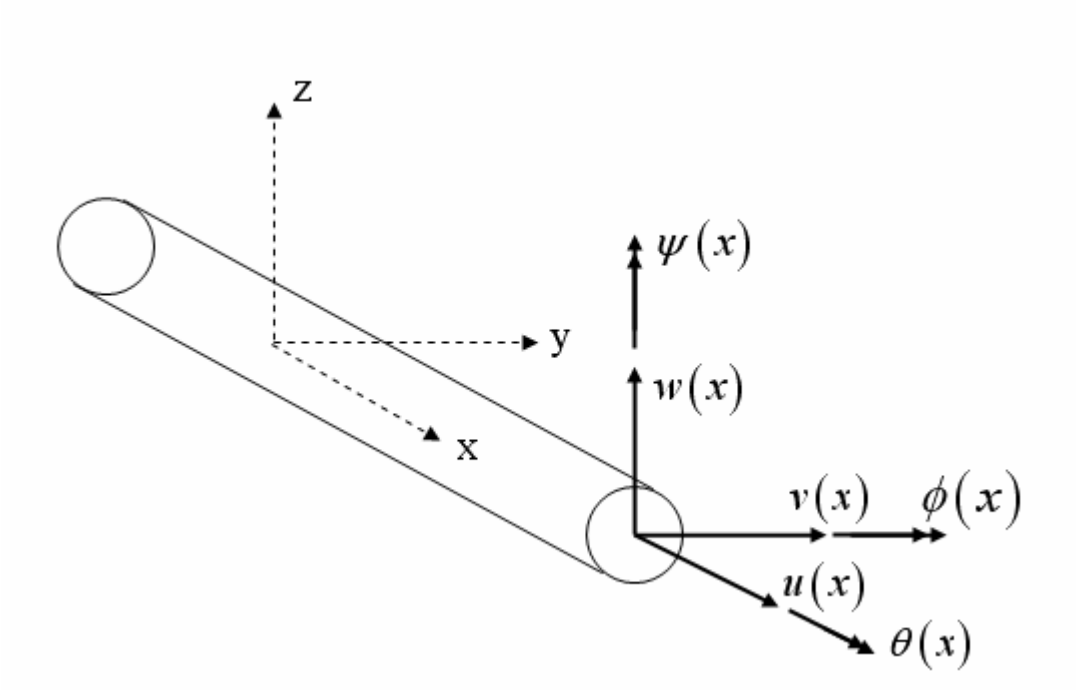

Figure – 2.2 Deformations and rotations of 3D Timoshenko beam

The axial action of the beam can be represented by deformation u.

Bending in xy plane can be represented by deformation v and rotation ψ.

Bending in xz plane can be represented by deformation w and rotation ϕ.

The torsional action of the beam can be represented by rotation θ.

The displacement of an arbitrary point in the beam can be expressed as:

$$U(x,y,z) = u(x) + z\phi(x) - y\psi(x) \tag{2.8}$$

$$V(x,y,z) = v(x) - z\theta(x) \tag{2.9}$$

$$W(x,y,z) = w(x) + y\theta(x) \tag{2.10}$$

Differentiation of the equations above gives the strain fields,

$$\varepsilon_{xx} = u_{,x} + z\phi_{,x} - y\psi_{,x} \tag{2.11}$$

$$\gamma_{xy} = v_{,x} - \psi - z\theta_{,x} \tag{2.12}$$

$$\gamma_{zx} = w_{,x} + \phi + y\theta_{,x} \tag{2.13}$$

$$\varepsilon_{yy} = \varepsilon_{zz} = \gamma_{yz} = 0 \tag{2.14}$$

Then stresses can be expressed as,

$$\sigma_{xx} = E\left(u_{,x} + z\phi_{,x} - y\psi_{,x}\right) \tag{2.15}$$

$$\sigma_{xy} = G\left(v_{,x} - \psi - z\theta_{,x}\right) \tag{2.16}$$

$$\sigma_{zx} = G\left(w_{,x} + \phi + y\theta_{,x}\right) \tag{2.17}$$

$$\sigma_{yy} = \sigma_{zz} = \sigma_{yz} = 0 \tag{2.18}$$

The stress resultants can be obtained by integrating stresses over the cross-section as,

$$F_x = \int_A \sigma_{xx} dA = EA(x)u_{,x} \tag{2.19}$$

$$F_y = \int_A \sigma_{xy} dA = kGA(x)\left(v_{,x} - \psi\right) \tag{2.20}$$

$$F_z = \int_A \sigma_{xz} dA = kGA(x)\left(w_{,x} + \phi\right) \tag{2.21}$$

$$M_x = \int_A \left(y\sigma_{xz} - z\sigma_{xy}\right) dA = GJ(x)\theta_{,x} \tag{2.22}$$

$$M_y = \int_A z\sigma_{xx} dA = -EI_{yz}(x)\psi_{,x} + EI_{yy}(x)\phi_{,x} \tag{2.23}$$

$$M_z = \int_A y\sigma_{xx} dA = -EI_{yz}(x)\phi_{,x} + EI_{zz}(x)\psi_{,x} \tag{2.24}$$

where $\int ydA = \int zdA = 0$ and k is shear correction factor.

Solving for $\phi_{,x}$ and $\psi_{,x}$ from equations 2.23 and 2.24,

$$\phi_{,x} = \frac{M_y I_{zz}(x) + M_z I_{yz}(x)}{E\left(I_{yy}(x)I_{zz}(x) - I_{yz}(x)^2\right)} \tag{2.25}$$

$$\phi_{,x} = \frac{M_y I_{yz}(x) + M_z I_{yy}(x)}{E\left(I_{yy}(x)I_{zz}(x) - I_{yz}(x)^2\right)} \tag{2.26}$$

It can be recognized that all the cross-sectional properties are expressed as functions of x. For simple geometries such as rectangular beams the variation of cross-sectional properties can be represented by exact functions without any cause of complexity in kinematic equations.

For tapered beams which have linearly varying depth and constant width, Gupta [2] represent variation of area and inertia by approximate functions involving shape factors. This method shall be used for complex geometries such as I beam to simplify the equations of kinematics which are utilized in hybrid stress formulations.

Tapered beam geometry is given in Figure 2.3,

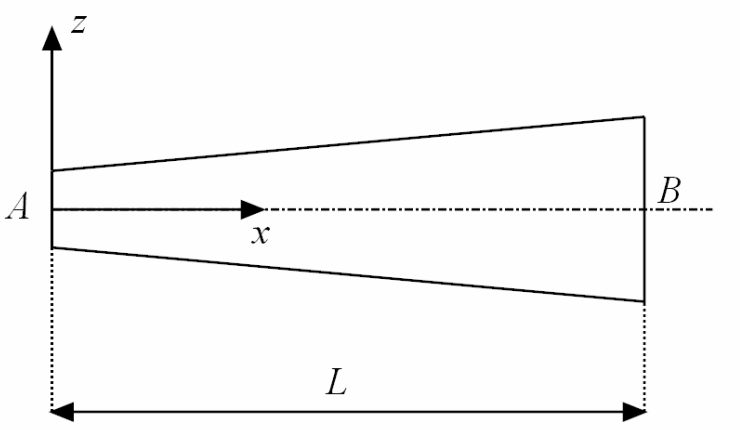

Figure – 2.3 Geometry of tapered beam

The smaller end of the beam is denoted as end A and larger end as B. The depth of the cross section at ends A and B are d_a and d_b, respectively. The length of the element is L.

For most of the beam shapes the variation of cross-sectional properties shall be represented as,

$$A(x) = A_a\left(1 + r\frac{x}{L}\right)^m \tag{2.27}$$

$$I_{yy}(x) = I_{yya}\left(1 + r\frac{x}{L}\right)^n \tag{2.28}$$

$$I_{zz}(x) = I_{zza}\left(1 + r\frac{x}{L}\right)^p \tag{2.29}$$

$$I_{yz}(x) = I_{yza}\left(1 + r\frac{x}{L}\right)^s \tag{2.30}$$

$$J(x) = J_a\left(1 + r\frac{x}{L}\right)^t \tag{2.31}$$

where,

$$r = \frac{d_b}{d_a} - 1$$

and shape factors m, n, p, s, t are,

$$m = \frac{\log\left(\frac{A_b}{A_a}\right)}{l\,\mathrm{og}\left(\frac{d_b}{d_a}\right)} - 1 \qquad n = \frac{\log\left(\frac{I_{yyb}}{I_{yya}}\right)}{l\,\mathrm{og}\left(\frac{d_b}{d_a}\right)} - 1$$

$$p = \frac{\log\left(\frac{I_{zzb}}{I_{zza}}\right)}{l\,\mathrm{og}\left(\frac{d_b}{d_a}\right)} - 1 \qquad s = \frac{\log\left(\frac{I_{yzb}}{I_{yza}}\right)}{l\,\mathrm{og}\left(\frac{d_b}{d_a}\right)} - 1$$

$$t = \frac{\log\left(\frac{J_b}{J_a}\right)}{l\,\mathrm{og}\left(\frac{d_b}{d_a}\right)} - 1$$

2.2 Equilibrium Equations

Consider an infinitesimally small section of a beam element in Figure 2.4.

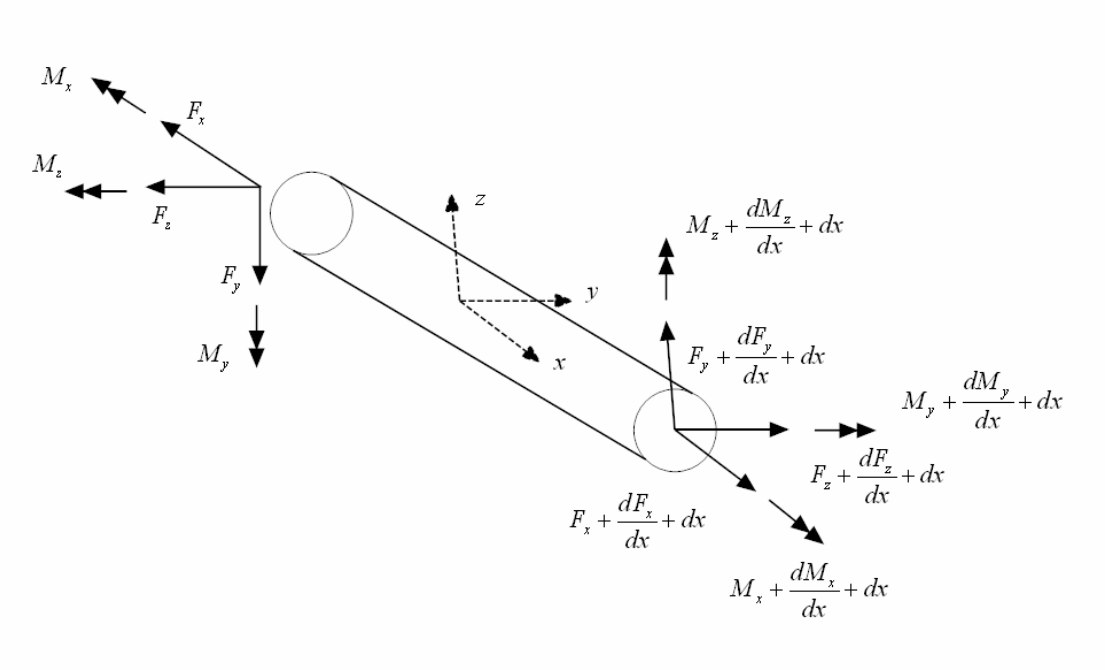

Figure – 2.4 Equilibrium of forces in a small beam element

The following homogenous equations are derived,

$$\sum F_x = 0 \qquad -F_x + F_x + \frac{dF_x}{dx}dx = 0 \quad \rightarrow \quad F_{x,x} = 0 \tag{2.32}$$

$$\sum F_y = 0 \qquad -F_y + F_y + \frac{dF_y}{dx}dx = 0 \quad \rightarrow \quad F_{y,x} = 0 \tag{2.33}$$

$$\sum F_z = 0 \qquad -F_z + F_z + \frac{dF_z}{dx}dx = 0 \quad \rightarrow \quad F_{z,x} = 0 \tag{2.34}$$

$$\sum M_x = 0 \qquad -M_x + M_x + \frac{dM_x}{dx}dx = 0 \quad \rightarrow \quad M_{x,x} = 0 \tag{2.35}$$

$$\sum M_y = 0 \qquad -M_y - F_z dx + M_y + \frac{dM_y}{dx}dx = 0 \quad \rightarrow \quad M_{y,x} - F_z = 0 \tag{2.36}$$

$$\sum M_z = 0 \qquad -M_z - F_y dx + M_z + \frac{dM_z}{dx}dx = 0 \quad \rightarrow \quad M_{z,x} - F_y = 0 \tag{2.37}$$

CHAPTER 3

FINITE ELEMENT FORMULATION

3.1 Hybrid Stress Formulation

Hybrid stress formulation consists of the variation of two-field complementary energy function. Two independent fields necessitate two independent assumptions for displacement field, u and stress field, σ.

Choose a stress field $\sigma = P \cdot B$ such that,

$$\sigma_{ij,j} = 0 \tag{3.1}$$

Choose a displacement field such that

$$d = N \cdot q \tag{3.2}$$

Then the strain field becomes $\varepsilon = B \cdot q$ and potential can be written as,

$$\prod = \int_V \left(\beta^T P^T B q - \frac{1}{2} \beta^T P^T S P \beta \right) dV - \int_{ST} q^T N^T T ds \tag{3.3}$$

Then the terms can be defined as,

$$G = \int_V P^T B dV \tag{3.4}$$

$$H = \int_V P^T S P^T dV \tag{3.5}$$

$$F = \int_{ST} N^T T P^T ds \tag{3.6}$$

By employing expressions 3.4, 3.5 and 3.6 to equation 3.3,

$$\prod = \beta^T G q - \frac{1}{2}\beta^T H \beta - q^T F \tag{3.7}$$

$\prod$ is minimized by $\frac{\partial \prod}{\partial \beta} = 0$ and $\frac{\partial \prod}{\partial q} = 0$. Then β can be found as,

$$\beta = H^{-1} G q \tag{3.8}$$

and the equation 3.7 reduces to,

$$\prod = \frac{1}{2} q^T G^T H^{-1} G q - q^T F \tag{3.9}$$

Define $k = G^T H^{-1} G$ (3.10)

$\prod$ becomes $\prod = \frac{1}{2} q^T k q - q^T F$

By $\frac{\partial \prod}{\partial q^T} = 0$, the well known equation "$kq = F$" can be obtained.

Assume stress field to satisfy equilibrium equations stated in Section 2.2:

$$F_x = \beta_1 \qquad T = \beta_4$$
$$F_y = \beta_2 \qquad M_y = \beta_5 + \beta_3 x$$
$$F_z = \beta_3 \qquad M_z = \beta_6 - \beta_2 x \tag{3.11}$$

Then $\sigma' = P\beta$ and in open form,

$$\begin{pmatrix} F_x \\ F_y \\ F_z \\ T \\ M_y \\ M_z \end{pmatrix} = \begin{pmatrix} 1 & 0 & 0 & 0 & 0 & 0 \\ 0 & 1 & 0 & 0 & 0 & 0 \\ 0 & 0 & 1 & 0 & 0 & 0 \\ 0 & 0 & 0 & 1 & 0 & 0 \\ 0 & 0 & x & 0 & 1 & 0 \\ 0 & -x & 0 & 0 & 0 & 1 \end{pmatrix} \beta$$

Force displacement relations in the matrix form can be written from the force-displacement relations derived in the section 2.1 as:

$$r = S\varepsilon$$

$$\begin{pmatrix} F_x \\ F_y \\ F_z \\ T \\ M_y \\ M_z \end{pmatrix} = \begin{pmatrix} EA(x) & 0 & 0 & 0 & 0 & 0 \\ 0 & kGA(x) & 0 & 0 & 0 & 0 \\ 0 & 0 & kGA(x) & 0 & 0 & 0 \\ 0 & 0 & 0 & GJ(x) & 0 & 0 \\ 0 & 0 & 0 & 0 & EI_y(x) & -EI_{yz}(x) \\ 0 & 0 & 0 & 0 & -EI_{yz}(x) & EI_z(x) \end{pmatrix} \begin{pmatrix} u_{,x} \\ v_{,x} - \psi \\ w_{,x} + \phi \\ \theta_{,x} \\ \phi_{,x} \\ \psi_{,x} \end{pmatrix}$$

The strain energy in terms of stress resultant is:

$$\prod = \frac{1}{2} \beta^T H \beta \tag{3.12}$$

The boundary traction can be expressed as,

$$\begin{pmatrix} F_{x_1} \\ F_{y_1} \\ F_{z_1} \\ T_1 \\ M_{y_1} \\ M_{z_1} \\ F_{x_2} \\ F_{y_2} \\ F_{z_2} \\ T_1 \\ M_{y_2} \\ M_{z_2} \end{pmatrix} = \begin{pmatrix} -1 & 0 & 0 & 0 & 0 & 0 \\ 0 & -1 & 0 & 0 & 0 & 0 \\ 0 & 0 & -1 & 0 & 0 & 0 \\ 0 & 0 & 0 & -1 & 0 & 0 \\ 0 & 0 & 0 & 0 & -1 & 0 \\ 0 & 0 & 0 & 0 & 0 & -1 \\ 1 & 0 & 0 & 0 & 0 & 0 \\ 0 & 1 & 0 & 0 & 0 & 0 \\ 0 & 0 & 1 & 0 & 0 & 0 \\ 0 & 0 & 0 & 1 & 0 & 0 \\ 0 & 0 & L & 0 & 1 & 0 \\ 0 & -L & 0 & 0 & 0 & 1 \end{pmatrix} \cdot \begin{pmatrix} \beta_1 \\ \beta_2 \\ \beta_3 \\ \beta_4 \\ \beta_5 \\ \beta_6 \end{pmatrix}$$

The 12*6 matrix in above denotes G matrix in equation 3.10.

3.2 Element Mass and Geometric Stiffness Matrices

For elostodynamic problems with initial stress, hybrid stress functional can be represented as:

$$\Pi = \int_{t_1}^{t_2} \left[\int_V \left(\beta^T P^T B q - \frac{1}{2} \beta^T P^T S P \beta \frac{1}{2} \rho \dot{q}^T N^T N \dot{q} + \frac{1}{2} q^T A^T \sigma_0 A q \right) dV - \int_{ST} q^T N^T T dS \right] dt$$

Using equations 3.4, 3.5, 3.6, 3.8, 3.10 and defining,

Mass matrix:

$$m = \int_V \rho N^T N dV \tag{3.13}$$

Geometric stiffness matrix:

$$k_G = \int_V A^T \sigma_0 A dV \tag{3.14}$$

The functional can be represented as:

$$\Pi = \int_{t_1}^{t_2} \left(\frac{1}{2} q^T k q - \frac{1}{2} \dot{q}^T m \dot{q} + \frac{1}{2} q^T k_G q - q^T F \right) dt \tag{3.15}$$

This functional is dependent on time thus using Lagrange equation:

$$\frac{d}{dt}\left(\frac{\partial \Pi}{\partial \dot{q}} \right) - \frac{\partial \Pi}{\partial q} = 0$$

Well known formulation for dynamic and stability analysis has been found:

$$m\ddot{q} + \left(k + k_G\right)q = F \tag{3.16}$$

By solving the linear eigenvalue problem of equation 3.16 critical buckling loads and lateral free vibration modes for an elastic body can be obtained.

Functions for displacement and rotation:

Displacement and rotation functions can be determined exactly from the equilibrium equations and kinematic of deformations which are obtained in sections 2.1 and 2.2.

xy bending

From equations 2.20 and 3.11

$$v_{,x} - \psi = \frac{F_y}{kGA(x)} = \frac{\beta_2}{kGA(x)} \tag{3.17}$$

$$\begin{aligned}\psi_{,x} &= \frac{M_z I_{yy}(x)}{E\left(I_{yy}(x)I_{zz}(x) - I_{yz}(x)^2\right)} + \frac{M_y I_{yz}(x)}{E\left(I_{yy}(x)I_{zz}(x) - I_{yz}(x)^2\right)} \\ \psi_{,x} &= \frac{\left(\beta_5 + \beta_3 x\right)I_{yy}(x)}{E\left(I_{yy}(x)I_{zz}(x) - I_{yz}(x)^2\right)} + \frac{\left(\beta_6 - \beta_2 x\right)I_{yz}(x)}{E\left(I_{yy}(x)I_{zz}(x) - I_{yz}(x)^2\right)}\end{aligned} \tag{3.18}$$

Differentiate equation 3.17 once,

$$v_{,xx} - \psi_{,x} = \frac{\partial}{\partial x}\left(\frac{\beta_2}{kGA(x)}\right) \tag{3.19}$$

By putting equation 3.18 into equation 3.19, one can obtain $v_{,xx}$:

$$v_{,xx} = \frac{(\beta_5 + \beta_3 x) I_{yy}(x)}{E\left(I_{yy}(x) I_{zz}(x) - I_{yz}(x)^2\right)} + \frac{(\beta_6 - \beta_2 x) I_{yz}(x)}{E\left(I_{yy}(x) I_{zz}(x) - I_{yz}(x)^2\right)} + \frac{\partial}{\partial x}\left(\frac{\beta_1}{kGA(x)}\right) \quad (3.20)$$

Integrating equation 3.21 twice gives the function of transverse displacement in y direction,

$$v = \iint\left(\frac{(\beta_5 + \beta_3 x) I_{yy}(x)}{E\left(I_{yy}(x) I_{zz}(x) - I_{yz}(x)^2\right)} + \frac{(\beta_6 - \beta_2 x) I_{yz}(x)}{E\left(I_{yy}(x) I_{zz}(x) - I_{yz}(x)^2\right)} + \frac{\partial}{\partial x}\left(\frac{\beta_2}{kGA(x)}\right)\right)dx + c_1 x + c_2$$

Define,

$$\Delta = \iint\left(\frac{(\beta_5 + \beta_3 x) I_{yy}(x)}{E\left(I_{yy}(x) I_{zz}(x) - I_{yz}(x)^2\right)} + \frac{(\beta_6 - \beta_2 x) I_{yz}(x)}{E\left(I_{yy}(x) I_{zz}(x) - I_{yz}(x)^2\right)} + \frac{\partial}{\partial x}\left(\frac{\beta_2}{kGA(x)}\right)\right)dx$$

(3.21)

For x=0

$$v(0) = v_1 = c_2 + \Delta(0) \qquad \Rightarrow \qquad c_2 = v_1 - \Delta(0)$$

For x=L

$$v(L) = v_2 = c_1 L + v_1 - \Delta(0) + \Delta(L) \quad \Rightarrow \quad c_1 = \frac{v_2 - v_1 + \Delta(L) - \Delta(0)}{L}$$

Beta values can be expressed in terms of degrees of freedom at two nodes of the element using equation 3.8;

$$\begin{pmatrix} \beta_1 \\ \beta_2 \\ \beta_3 \\ \beta_4 \\ \beta_5 \\ \beta_6 \end{pmatrix} = \left(H^{-1}G\right)_{6\times 12} \begin{pmatrix} u_1 \\ v_1 \\ w_1 \\ \theta_1 \\ \phi_1 \\ \psi_1 \\ u_2 \\ v_2 \\ w_2 \\ \theta_2 \\ \phi_2 \\ \psi_2 \end{pmatrix} \tag{3.22}$$

If beta expressions in equation 3.22 are substituted in transverse displacement function with c_1 and c_2 constants, transverse displacement v through out the beam element can be obtained in terms of degrees of freedom and variable x.

In general form,

$$v = f^{v}{}_{1}(x)v_1 + f^{v}{}_{2}(x)w_1 + f^{v}{}_{3}(x)\phi_1 + f^{v}{}_{4}(x)\psi_1 + f^{v}{}_{5}(x)v_2 + f^{v}{}_{6}(x)w_2 + f^{v}{}_{7}(x)\phi_2 + f^{v}{}_{8}(x)\psi_2 \tag{3.23}$$

Back to equation 3.17,

$$v_{,x} - \psi = \frac{\beta_2}{kGA(x)} \Rightarrow \psi = v_{,x} - \frac{\beta_2}{kGA(x)}$$

Substituting 3.23 into above equation gives the rotation ψ in terms of nodal degrees of freedom and variable x.

$$\psi = f^{\psi}{}_1(x)v_1 + f^{\psi}{}_2(x)w_1 + f^{\psi}{}_3(x)\phi_1 + f^{\psi}{}_4(x)\psi_1 + f^{\psi}{}_5(x)v_2 + f^{\psi}{}_6(x)w_2 + f^{\psi}{}_7(x)\phi_2 + f^{\psi}{}_8(x)\psi_2$$

(3.24)

xz bending:

From equations 2.21 and 3.11

$$w_{,x} + \phi = \frac{F_z}{kGA(x)} = \frac{\beta_3}{kGA(x)} \tag{3.25}$$

$$\begin{aligned} \phi_{,x} &= -\frac{M_z I_{zz}(x)}{E\left(I_{yy}(x)I_{zz}(x) - I_{yz}(x)^2\right)} - \frac{M_y I_{yz}(x)}{E\left(I_{yy}(x)I_{zz}(x) - I_{yz}(x)^2\right)} \\ \phi_{,x} &= -\frac{\left(\beta_6 - \beta_2 x\right) I_{yy}(x)}{E\left(I_{yy}(x)I_{zz}(x) - I_{yz}(x)^2\right)} - \frac{\left(\beta_5 + \beta_3 x\right) I_{yz}(x)}{E\left(I_{yy}(x)I_{zz}(x) - I_{yz}(x)^2\right)} \end{aligned} \tag{3.26}$$

Differentiate equation 3.26 once,

$$w_{,xx} + \phi_{,x} = \frac{\partial}{\partial x}\left(\frac{\beta_3}{kGA(x)}\right) \tag{3.27}$$

By putting equation 3.26 into equation 3.27, $w_{,xx}$ can be obtained:

$$w_{,xx} = -\frac{\left(\beta_6 - \beta_2 x\right) I_{yy}(x)}{E\left(I_{yy}(x)I_{zz}(x) - I_{yz}(x)^2\right)} - \frac{\left(\beta_5 + \beta_3 x\right) I_{yz}(x)}{E\left(I_{yy}(x)I_{zz}(x) - I_{yz}(x)^2\right)} + \frac{\partial}{\partial x}\left(\frac{\beta_3}{kGA(x)}\right) \tag{3.28}$$

Integrating equation 3.28 twice gives the function of transverse displacement in z direction,

$$w = \iint\left(-\frac{\left(\beta_6 - \beta_2 x\right) I_{yy}(x)}{E\left(I_{yy}(x) I_{zz}(x) - I_{yz}(x)^2\right)} - \frac{\left(\beta_5 + \beta_3 x\right) I_{yz}(x)}{E\left(I_{yy}(x) I_{zz}(x) - I_{yz}(x)^2\right)} + \frac{\partial}{\partial x}\left(\frac{\beta_2}{kGA(x)}\right)\right) dx + d_1 x + d_2$$

As in xy bending define,

$$\Delta = \iint\left(-\frac{\left(\beta_6 - \beta_2 x\right) I_{yy}(x)}{E\left(I_{yy}(x) I_{zz}(x) - I_{yz}(x)^2\right)} - \frac{\left(\beta_5 + \beta_3 x\right) I_{yz}(x)}{E\left(I_{yy}(x) I_{zz}(x) - I_{yz}(x)^2\right)} + \frac{\partial}{\partial x}\left(\frac{\beta_2}{kGA(x)}\right)\right) dx$$

(3.29)

For x=0

$$w(0) = w_1 = d_2 + \Delta(0) \qquad \Rightarrow \qquad d_2 = w_1 - \Delta(0)$$

For x=L

$$w(L) = w_2 = d_1 L + w_1 - \Delta(0) + \Delta(L) \quad \Rightarrow \quad d_1 = \frac{w_2 - w_1 + \Delta(L) - \Delta(0)}{L}$$

If beta expressions in equation 3.22 are substituted in transverse displacement function with d_1 and d_2 constants, transverse displacement w through out the beam element can be obtained in terms of degrees of freedom and variable x.

In general form,

$$w = f^{w}{}_1(x) v_1 + f^{w}{}_2(x) w_1 + f^{w}{}_3(x) \phi_1 + f^{w}{}_4(x) \psi_1 + f^{w}{}_5(x) v_2 + f^{w}{}_6(x) w_2 + f^{w}{}_7(x) \phi_2 + f^{w}{}_8(x) \psi_2$$

(3.30)

Back to equation 3.25

$$w_{,x} + \phi = \frac{F_z}{kGA(x)} = \frac{\beta_3}{kGA(x)}$$

Substituting 3.29 into above equation gives the ψ in terms of nodal degrees of freedom and variable x.

$$\phi = f^{\phi}{}_1(x)v_1 + f^{\phi}{}_2(x)w_1 + f^{\phi}{}_3(x)\phi_1 + f^{\phi}{}_4(x)\psi_1 + f^{\phi}{}_5(x)v_2 + f^{\phi}{}_6(x)w_2 + f^{\phi}{}_7(x)\phi_2 + f^{\phi}{}_8(x)\psi_2$$

(3.31)

Axial displacement and torsional rotation:

Axial displacement u and torsion rotation θ can be obtained via nodal degrees of freedom and variable x through out the beam element just as in xy and xz bending.

From equilibrium equations and kinematic of deformations in sections 2.1 and 2.2,

$$u_{,x} = \frac{F_x}{EA(x)} = \frac{\beta_1}{EA(x)} \tag{3.32}$$

$$\theta_{,x} = \frac{T}{GJ(x)} = \frac{\beta_4}{GJ(x)} \tag{3.33}$$

By integrating once:

$$u = \int \frac{\beta_1}{EA(x)} + e_1$$

$$\theta = \int \frac{\beta_4}{GJ(x)} + f_1$$

and employing the boundary conditions at x=0

$$e_1 = u_1 - \Delta(0)$$

$$f_1 = \theta_1 - \Delta(0)$$

where,

$$\Delta = \begin{cases} \int \dfrac{\beta_1}{EA(x)} & for\ u \\ \int \dfrac{\beta_4}{GJ(x)} & for\ \theta \end{cases} \tag{3.34}$$

By substituting beta values (equation 3.22) to axial displacement and torsional rotation functions with e_1 and f_1 constants, axial displacement u and torsional rotation θ can be obtained in terms of degrees of freedom and variable x:

$$u = f^{u}{}_1(x)u_1 + f^{u}{}_2(x)u_2 \tag{3.35}$$

$$\theta = f^{\theta}{}_1(x)\theta_1 + f^{\theta}{}_2(x)\theta_2 \tag{3.36}$$

Remember the displacement relations from section 2.1:

$$U(x,y,z) = u(x) + z\phi(x) - y\psi(x)$$

$$V(x,y,z) = v(x) - z\theta(x)$$

$$W(x,y,z) = w(x) + y\theta(x) \tag{3.37}$$

From equation 3.2, displacement field:

$$d = N \cdot q$$

By substituting terms $u, v, w, \theta, \phi, \psi$ in equation 3.37 by equations 3-23, 24, 30, 31, 35, 36; the matrix [N] can be obtained.

Mass matrix is

$$m = \int_V \rho N^T N dV \tag{3.38}$$

Geometric stiffness matrix is

$$k_G = \int_V A^T \sigma_0 A dV \tag{3.39}$$

where matrix [A] is derivative of matrix [N]

CHAPTER 4

STRUCTURE OF THE COMPUTER CODE

A code is generated in the Fortran Power Station environment to solve the finite element formulation derived at the previous sections. This code solves the nodal displacements and rotations, eigenvalues for buckling loads, eigenvalues for natural frequencies of free lateral vibration problem.

Structure matrices (element stiffness, geometric stiffness and mass matrices) are stored in vector form rather than in the square of bonded matrix form to save storage space by paper addressing of matrix elements which is known as skyline technique.

The code consists of one main code and five subroutines:

- MAIN.for
- PREP.for
- STFMAT.for
- ONEDIM.for
- ASMBLY.for
- COLSOL.for

4.1 Main.for

The analysis process is controlled by the main code by the following steps:

- Reads and stores the input data.

- Defines boundary conditions and creates necessary arrays which are used for implementation of the skyline technique by calling subroutine prep.for.
- Develops element stiffness, geometric stiffness and mass matrices by calling subroutine stfmat.for
- Stores the structure matrices in vector form to save storage space and assemble the global stiffness matrices by calling onedim.for and asmbly.for.
- Solves the static problem for displacements by calling colsol.for.
- For the stability and dynamic problems, finds the critical buckling loads and the natural frequencies by utilizing a linear eigenvalue solution algorithm.
- Outputs the requested results.

4.2 Prep.for

Subroutine prep.for defines the initial state of DOF's (degrees of freedom) at each node and creates necessary arrays which are used for implementation of the skyline technique.

4.3 Stfmat.for

Subroutine stfmat.for develops the element stiffness, geometric stiffness and mass matrices from the finite element formulations given in sections 3.1 and 3.2.The variation of the beam cross-sectional properties along the beam span and nodal displacement-rotation functions of equations given in section 3.2 are defined in this subroutine. The subroutine uses function numint for the numerical integration.

4.4 Onedim.for

Subroutine onedim.for stores the structure matrices in vector form to save storage space.

4.5 Assmbly.for

This subroutine assembles the global element, geometric stiffness and mass matrices of the entire beam structure.

4.6 Colsol.for

Subroutine colsol.for solves the linear systems of equations $kq = F$ by decomposition and backward substitution technique for the displacements of static problem.

Figures 4.1 and 4.2 show the solution algorithm of the finite element code and inverse iteration algorithm utilized for the linear eigenvalue solution respectively:

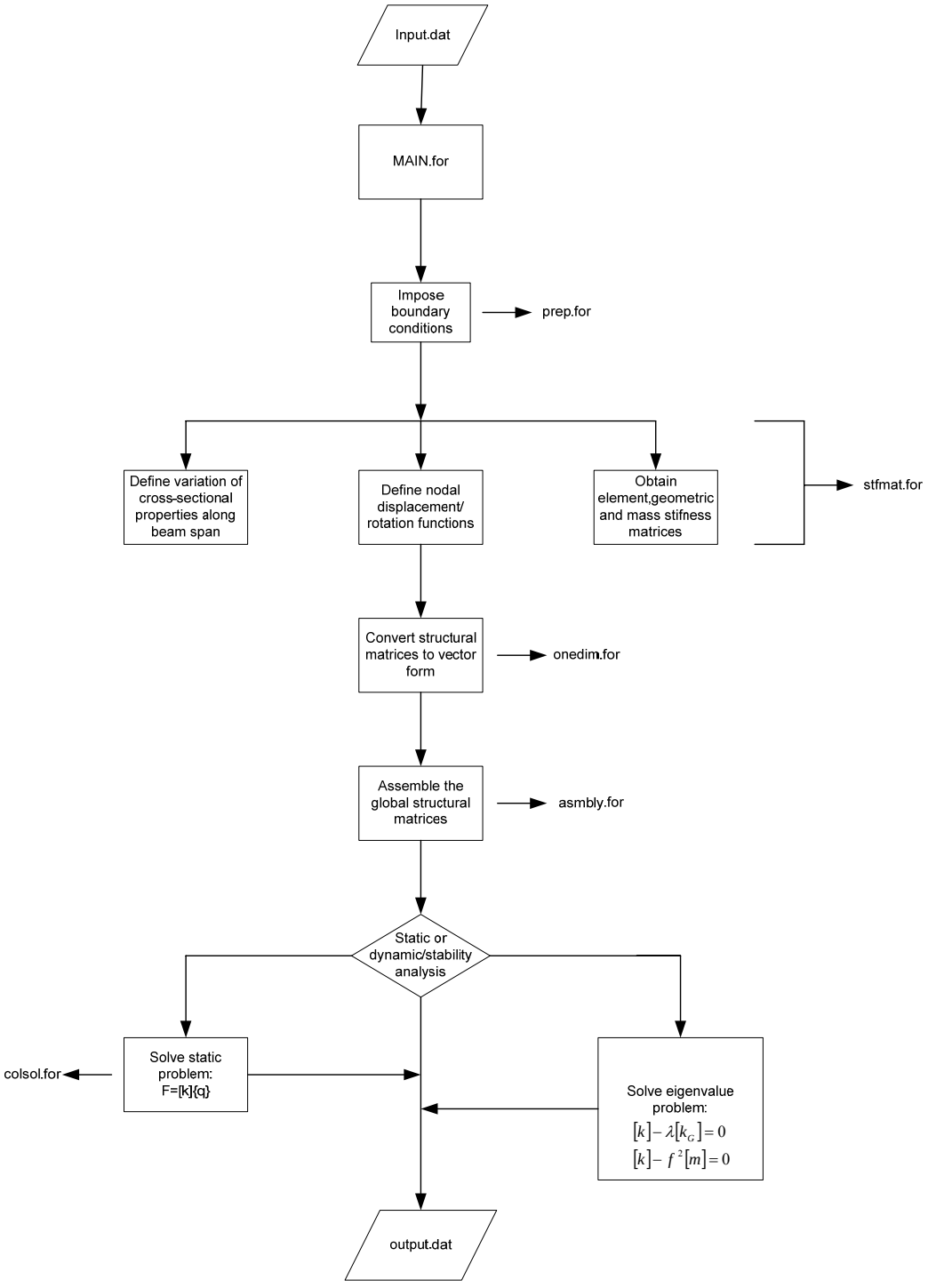

Figure – 4.1 Solution algorithm of the code

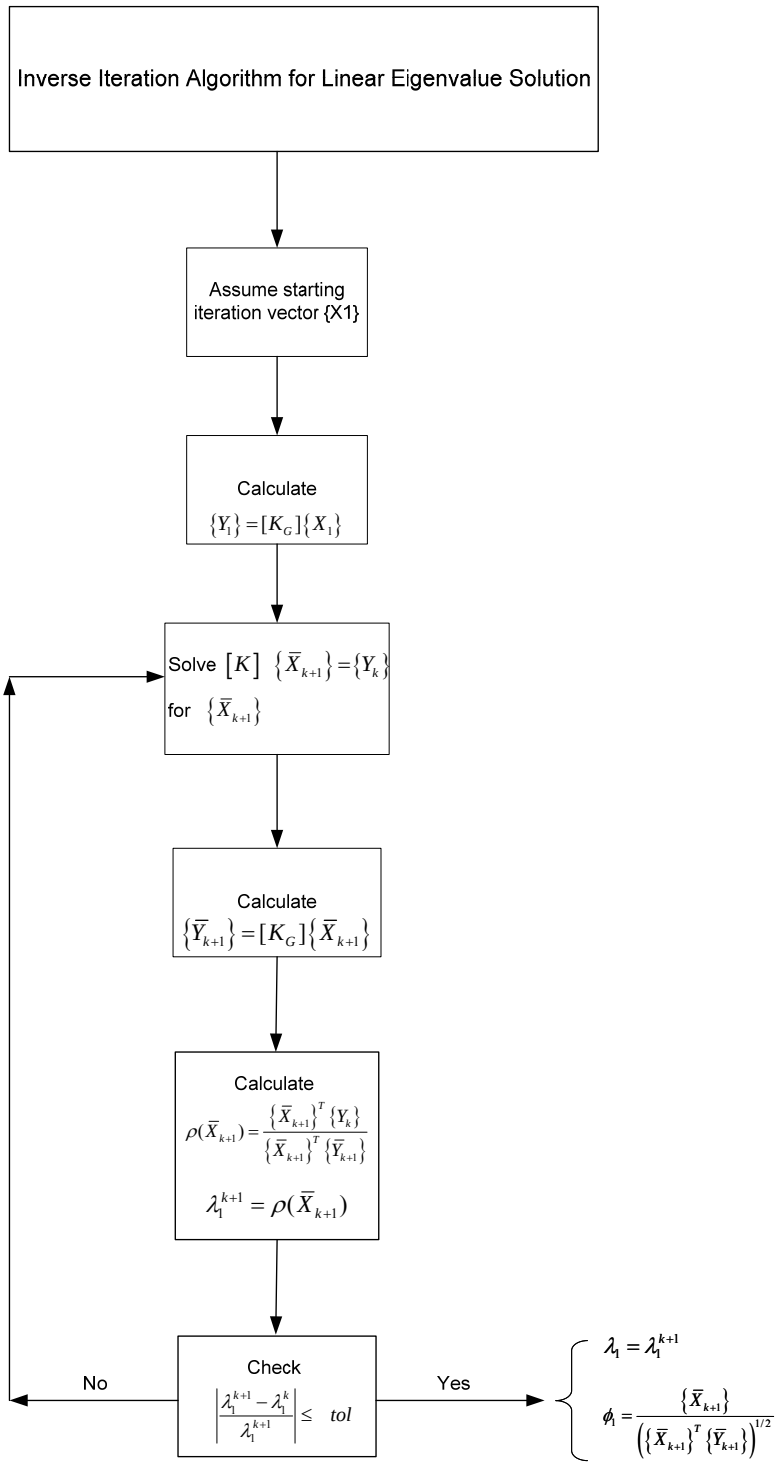

Figure – 4.2 Inverse iteration algorithm for linear eigenvalue solution

CHAPTER 5

CASE STUDIES

The element developed in this thesis is applied to number of test cases and problems. The test cases are to chosen to compare the elements results with the previously solved problems in the literature.

5.1 Rectangular Uniform Beam

In this analysis; a uniform beam with rectangular cross-sectional shape is investigated for:

1) Vertical displacement when subjected to unit transverse load.

2) Natural frequencies for free lateral vibration

3) Critical buckling load

The geometry and boundary conditions of the beam is given in Figure 5.1

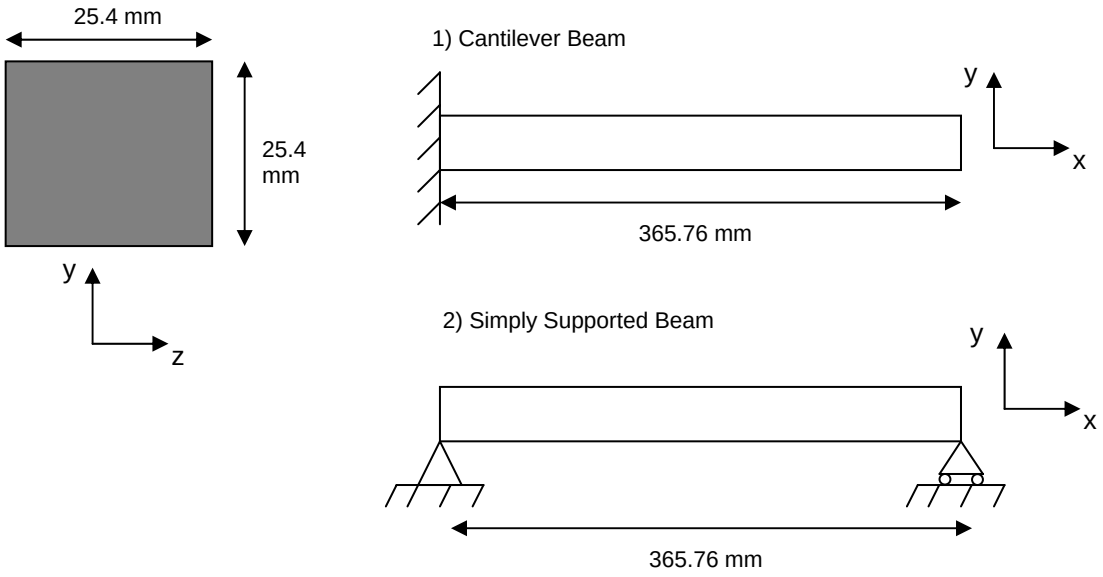

Figure – 5.1 The geometry and boundary conditions of uniform rectangular beam

Cross sectional properties of the beam in Figure 5.1 is given in Table 5.1:

Table 5.1 – Rectangular Beam Cross Sectional Properties

E (Mpa)	206840
G (Mpa)	77565
k	0.667
ρ (kg/m^3)	7757
Area (mm^2)	645.16
I_{yy} (mm^4)	34686
I_{zz} (mm^4)	34686
I_{yz} (mm^4)	0.

Tip-Loaded Cantilever Beam

A uniform cantilever beam of length L (365.76 mm) is fixed at x=0 and subjected to a transverse point force F (1 N) at x=L. The exact tip deflection and rotation is:

$$v_{(L)} = F \cdot (\frac{L^3}{3EI_{zz}} + \frac{L}{kGA}) = 2.284 \cdot 10^{-3}\ mm$$

$$\phi_{(L)} = \frac{FL^2}{2EI_{zz}} = 9.323 \cdot 10^{-6}\ rad$$

Results with single element solution for the present element at the tip:

$$v_{(L)} = 2.284 \cdot 10^{-3}\ mm$$

$$\phi_{(L)} = 9.323 \cdot 10^{-6}\ rad$$

Present formulation with single element solution yields exact tip deflection and rotation.

Free Vibration of Cantilever Beam

The lowest frequency of the cantilever beam with the properties given in Table 5.2 and Figure 5.1 are calculated. Table 5.1 shows the analytical solution, finite element solutions of Oral's (5) element and present element. In finite element computations a 16 element mesh is used.

Table 5.2 – Lowest Frequency (Hz) of cantilever beam (16 elements)

Analytical	Oral	Present
977	991	991

Present solution gives same results with Oral's anisoparametric hybrid element solution.

Free Vibration of Simply Supported Beam

The lowest natural frequency of a simply supported beam with properties given in Figure 5.1 and Table 5.1 are calculated using 20 elements. The results are presented in Table 5.3.

Table 5.3 – Nondimensional Frequency ($\frac{w_n}{\sqrt{EI_{zz}/\rho AL^4}}$) for first mode of cantilever beam (20 elements)

Analytical	Oral	Present
9.890	9.7843	9.7736

The result of the present solution is in good agreement with Oral's solution.

Stability of Simply Supported Beam

The critical load for simply supported beam with properties given in Figure 5.1 and Table 5.1 are calculated using 12 elements. The results are presented in Table 5.4.

$\frac{L}{r} = 50$ where $r = \sqrt{\frac{I_{zz}}{A}}$ (radius of gyration)

Table 5.4 – Critical Load (N) for simply supported beam (12 elements)

Analytical	Oral	Present
521026	518942	519085

The results for Oral and present solution slightly differs from Timoshenko's exact solution because of the fact that these two solutions include the effect of bending on axial deformation (rotary inertia).

5.2 Tip Deflection of Nonuniform Rectangular Beam

In this analysis, transverse tip deflection of the nonuniform rectangular cantilever beam with linearly varying height is analyzed. The beam is subjected to unit transverse load at the free edge of the beam. The geometry of the beam is shown in Figure 5.2

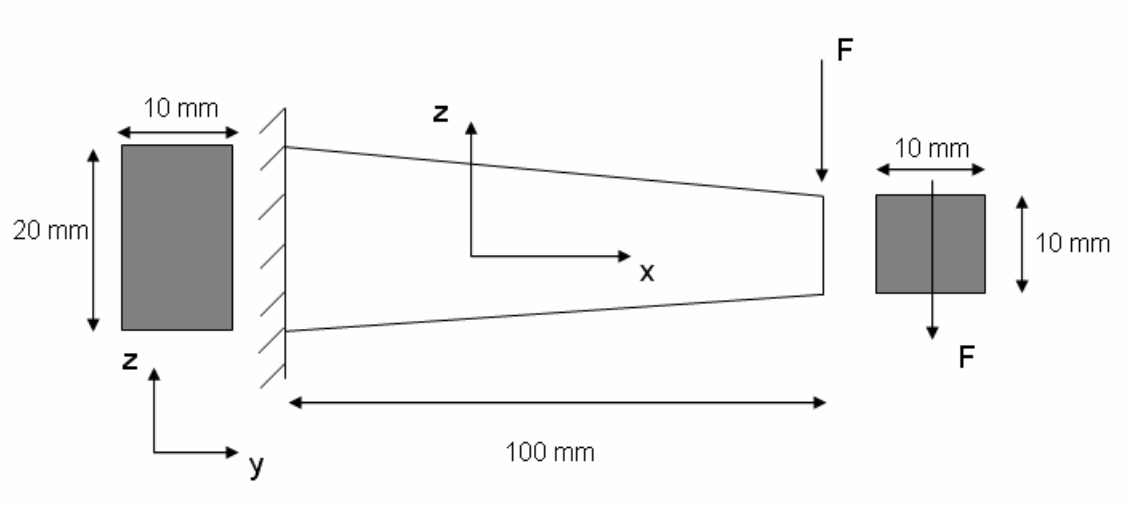

Figure – 5.2 The geometry of nonuniform rectangular beam of example 5.2

Material and cross-sectional properties are given below:

$E = 206000\,MPa$
$G = 79231\,MPa$
$\nu = 0.3$
$k = 0.833$

Table 5.5 gives result for vertical deflection at the tip for present single element solution, Friedman and Kosmatka (15) single Timoshenko beam element solution and exact Euler beam solution.

Table 5.5 – Tip deflection of nonuniform rectangular beam

Exact Euler Beam (15)	Timoshenko Beam (15)	Present
$3.97 \cdot 10^{-4}\ mm$	$4.07 \cdot 10^{-4}\ mm$	$4.10 \cdot 10^{-4}\ mm$

Figure 5.3 shows the deflection along the beam span of the example 5.2 for the present solution.

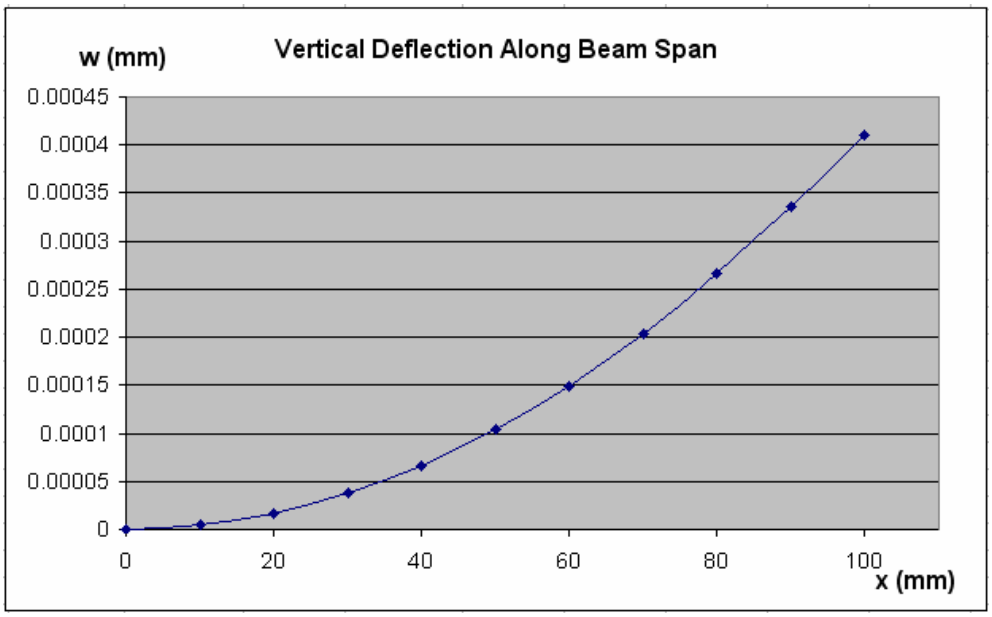

Figure – 5.3 Deflection of the nonuniform cantilever beam along the span

5.3 Tip Deflection of Nonuniform Circular Beam

The transverse tip deflection of the nonuniform circular cantilever beam with linearly varying diameter is analyzed. The beam is subjected to unit transverse load at the free edge of the beam. The geometry of the beam is shown in Figure 5.4

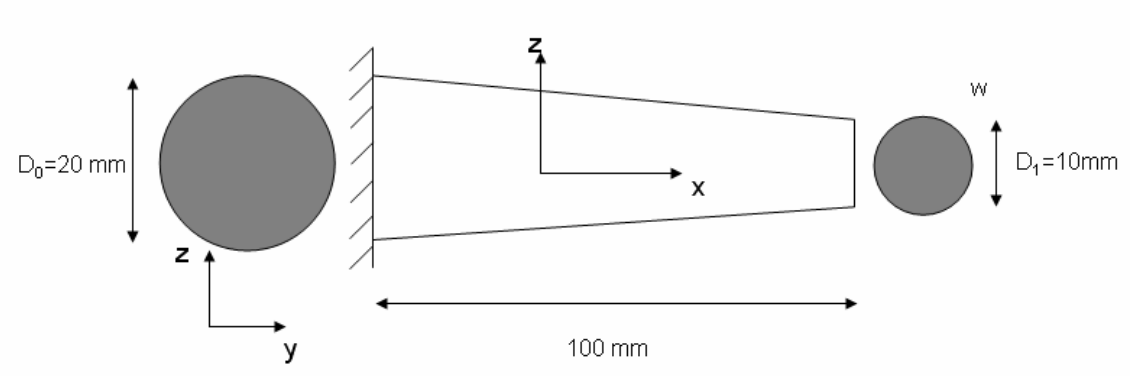

Figure – 5.4 The geometry of nonuniform circular beam

Material and cross-sectional properties are given below:

$E = 206000\,MPa$
$G = 79231\,MPa$
$\nu = 0.3$
$k = 0.9$

Table 5.6 gives result for vertical deflection at the tip for present element solution, Friedman and Kosmatka (15) Timoshenko beam element solution and exact Euler beam solution.

Table 5.6 – Tip deflection of nonuniform circular beam

Exact Euler Beam (15)	Timoshenko Beam (15)	Present
$1.65 \cdot 10^{-3}\ mm$	$1.68 \cdot 10^{-3}\ mm$	$1.66 \cdot 10^{-3}\ mm$

Present beam element solution is in good agreement with the Friedman and Kosmatka's beam element solution.

5.4 Free Vibration of Nonuniform Rectangular Beam - Example 1

In this analysis, natural frequencies for nonuniform rectangular Timoshenko beam are investigated. An example is solved to employ the element presented in the previous sections and results are compared with the results of Cleghorn & Tabarrok's (19) Timoshenko beam element solution. Beam has constant width and linearly varying height with clamped - clamped boundary condition as shown in Figure 5.5.

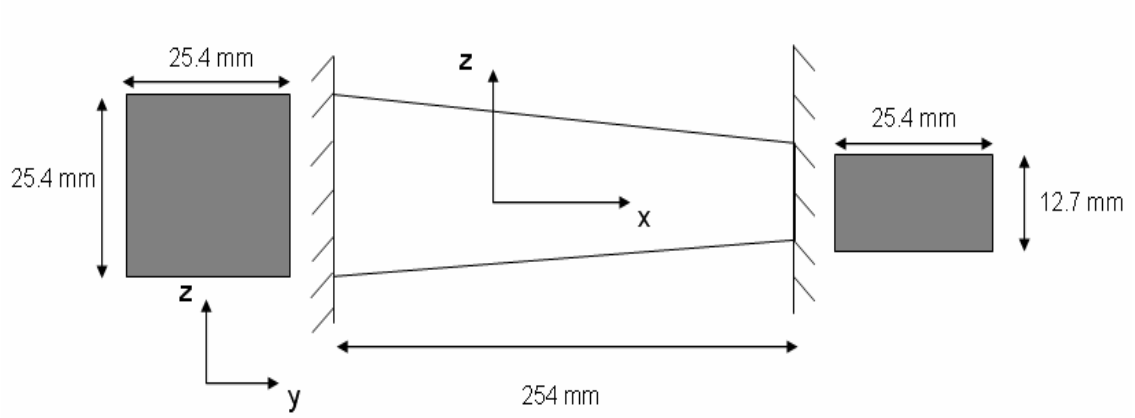

Figure – 5.5 Geometry and boundary conditions of nonuniform rectangular beam, free vibration example 1

Material properties are given below:

$E = 210000\,MPa$
$G = 80000\,MPa$
$\nu = 0.3$
$k = 0.667$
$\rho = 7825\,kg/m^3$

Results are compared with the results of Cleghorn & Tabarrok (19) Timoshenko beam finite element solutions in Table 5.7.

Table 5.7 – First natural modes (Hertz) of clamped-clamped nonuniform Timoshenko beam of rectangular cross-section

Number of elements	Cleghorn&Tabarrok (Hertz)	Present (Hertz)
2	9385.6	7767.3
3	9233.2	8233.4
4	9197.2	8521.4
5	9184.5	8680.1
6	9178.8	8770.5
7	9175.8	8824.7
8	9170.4	8858.5
9	9172.8	8880.1
10	9172	8894.5
11	9174.2	8904.3
12	9171	8911.1
13	9170.7	8915.9

Present solution gives poor results for small number of elements but has fast convergence while increasing number of elements and has closed results with Cleghorn & Tabarrok for 13 element solution. Convergence performance of Cleghorn & Tabbarrok solution and present solution is plotted in Figure 5.6.

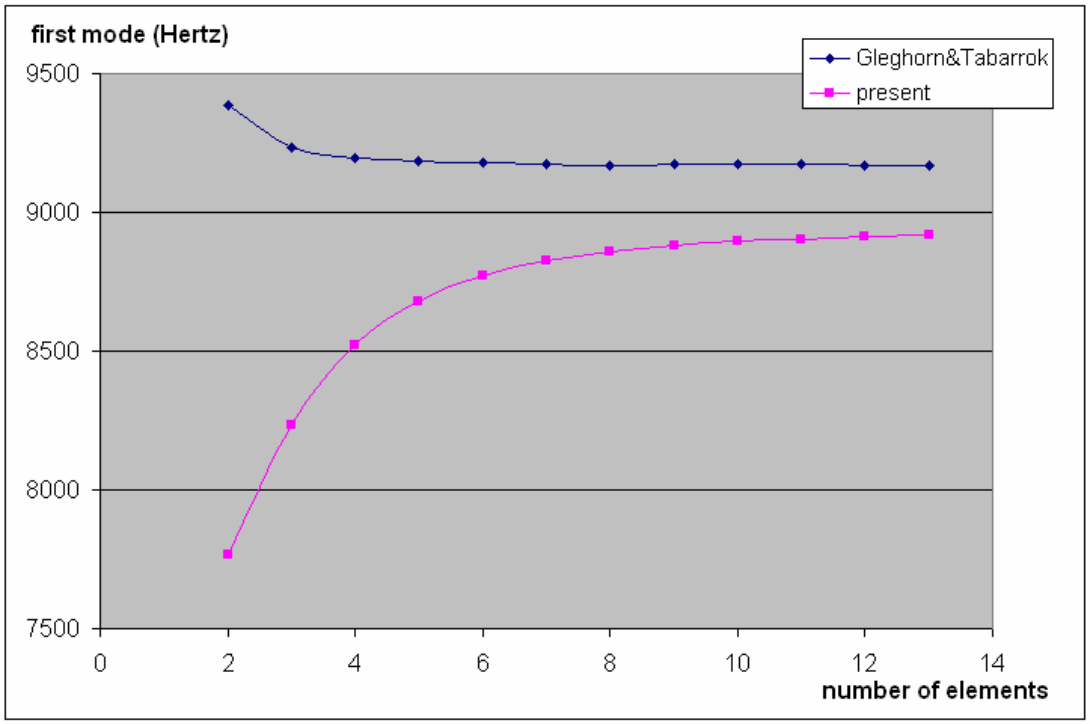

Figure – 5.6 Clamped – clamped nonuniform rectangular Timoshenko beam first mode as a function of number of elements

5.5 Free Vibration of Nonuniform Rectangular Beam - Example 2

In this analysis, natural frequencies for nonuniform rectangular Timoshenko beam are investigated for different boundary conditions and taper ratios. Beam has constant width and linearly varying height.

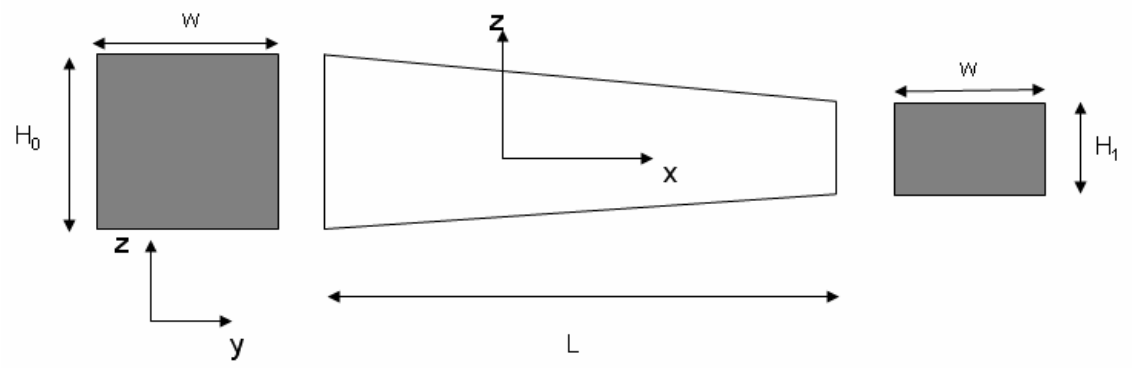

Figure – 5.7 Geometry of the nonuniform rectangular beam, free vibration example 2

Material properties are given below:

$E = 200000\,MPa$
$G = 76923\,MPa$
$\nu = 0.3$
$k = 0.833$
$\rho = 0.000007997\,kg \cdot s^2 / cm^4$

Results for different geometric parameters (α and r_0) are obtained with present six element solution and compared with Rossi & Laura's (22) Timoshenko beam ten element solution.

where;

$$\alpha = \frac{H_1}{H_0} - 1 \text{ and } r_0 = \sqrt{\frac{I_0}{A_0}}$$

Table 5.8 – Nondimensional natural modes $\left(\sqrt{\frac{\rho A_0}{EI_0}} \cdot \omega \cdot L^2\right)$ of rectangular beam for different boundary conditions and geometric parameters

	$\frac{r_0}{L} = 0.05$						$\frac{r_0}{L} = 0.1$					
	$\alpha = 0.1$		$\alpha = 0.2$		$\alpha = 0.3$		$\alpha = 0.1$		$\alpha = 0.2$		$\alpha = 0.3$	
	Present	Rossi & Laura	Present	Rossi & Laura	Present	Rossi & Laura	Present	Rossi & Laura	Present	Rossi & Laura	Present	Rossi & Laura
C-F	3.295	3.396	3.259	3.361	3.225	3.330	3.082	3.184	3.041	3.145	3.005	3.109
F-C	3.700	3.806	4.063	4.177	4.426	4.549	3.433	3.543	3.735	3.852	4.029	4.154
SS-SS	9.542	9.829	9.928	10.228	10.294	10.610	8.416	8.683	8.680	8.954	8.923	9.205
C-SS	13.715	14.232	14.045	14.587	14.350	14.920	10.866	11.245	11.001	11.387	11.119	11.511
SS-C	14.063	14.570	14.728	15.251	15.361	15.899	11.098	11.471	11.449	11.825	11.769	12.148
C-C	18.680	19.486	19.266	20.094	19.814	20.665	13.614	14.089	13.840	14.316	14.042	14.518

Results of present Timoshenko beam element is in good agreement with Rosa and Laura's Timoshenko beam element.

Figure 5.8 shows convergence performance of present beam element for geometric parameters: $\frac{r_0}{L} = 0.05$, $\alpha = 0.1$ and boundary condition: clamped - free.

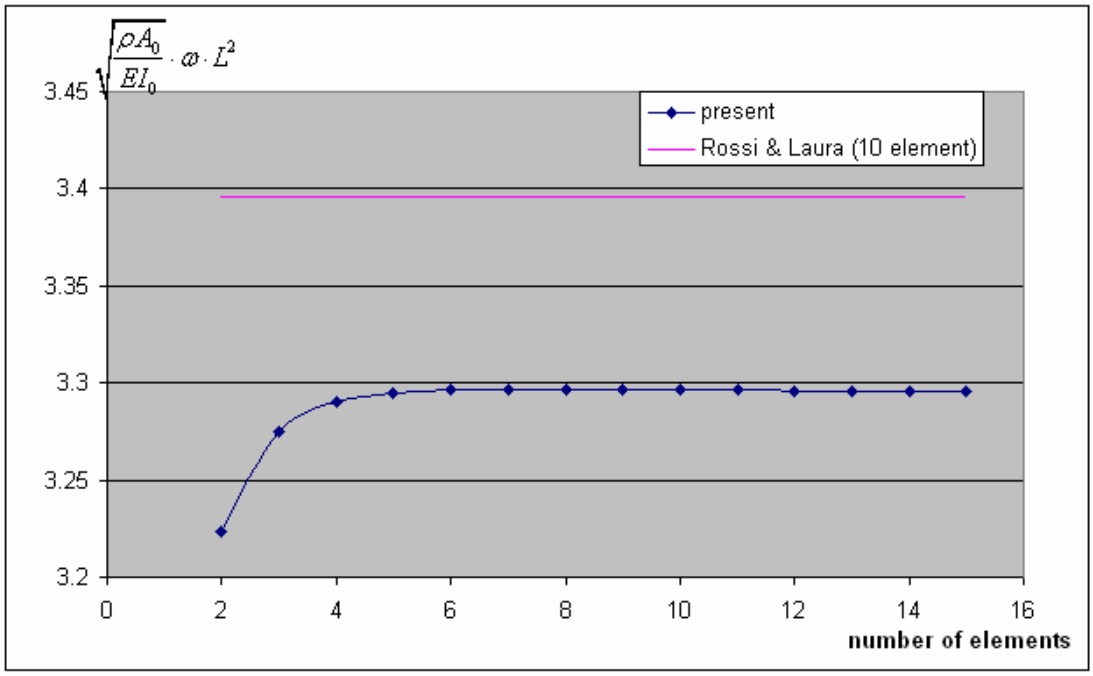

Figure – 5.8 Cantilever nonuniform rectangular beam first mode as a function of number of elements

5.6 Buckling of Nonuniform Rectangular Beam - Example 1

In this analysis critical buckling loads for nonuniform rectangular Timoshenko beam are examined for various boundary conditions. The results are compared with the results which are obtained from MSC/NASTRAN quad element solution.

Beam has constant width and varying height as shown in Figure 5.9.

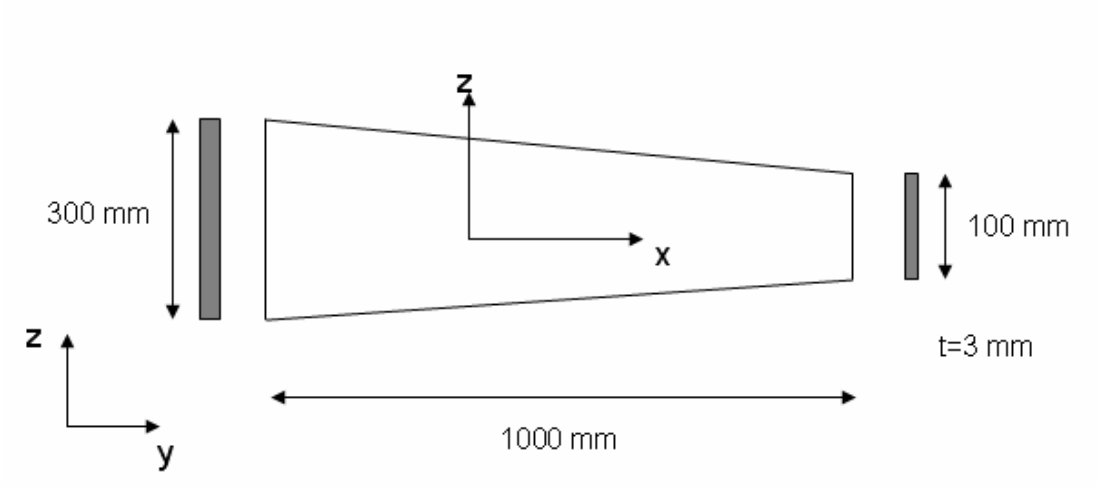

Figure – 5.9 Geometry of nonuniform rectangular beam, buckling example 1

Material properties are given below:

$E = 210000\,MPa$
$G = 80000\,MPa$
$\nu = 0.3$
$k = 0.833$

Results of present 4 element solution are compared with the MSC/NASTRAN 30*10 quad element solution in Table 5.9.

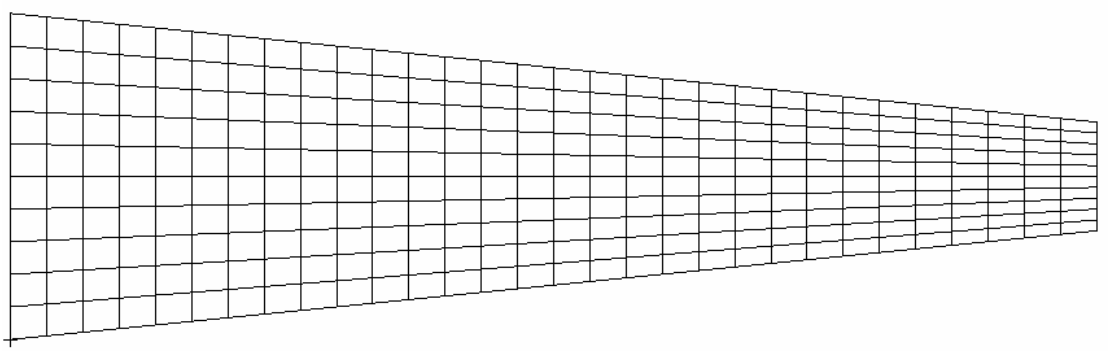

Figure – 5.10 NASTRAN 30*10 quad element nonuniform beam model

Table 5.9 –Critical buckling loads for nonuniform rectangular cross-section beam of example 1.

BC	Nastran 30*10 element solution (N)	Present 4 element solution (N)
Simply Supported-Simply Supported	892.28	873.30
Clamped-Free	272.44	264.26
Clamped-Clamped	3578.30	3423.38

Results of present solution are in good agreement with the MSC NASTRAN solutions.

Figure 5.11 shows the present element convergence for simply supported beam problem. From the figure it is clear that after four elements critical buckling load values converges to that of MSC/NASTRAN solution.

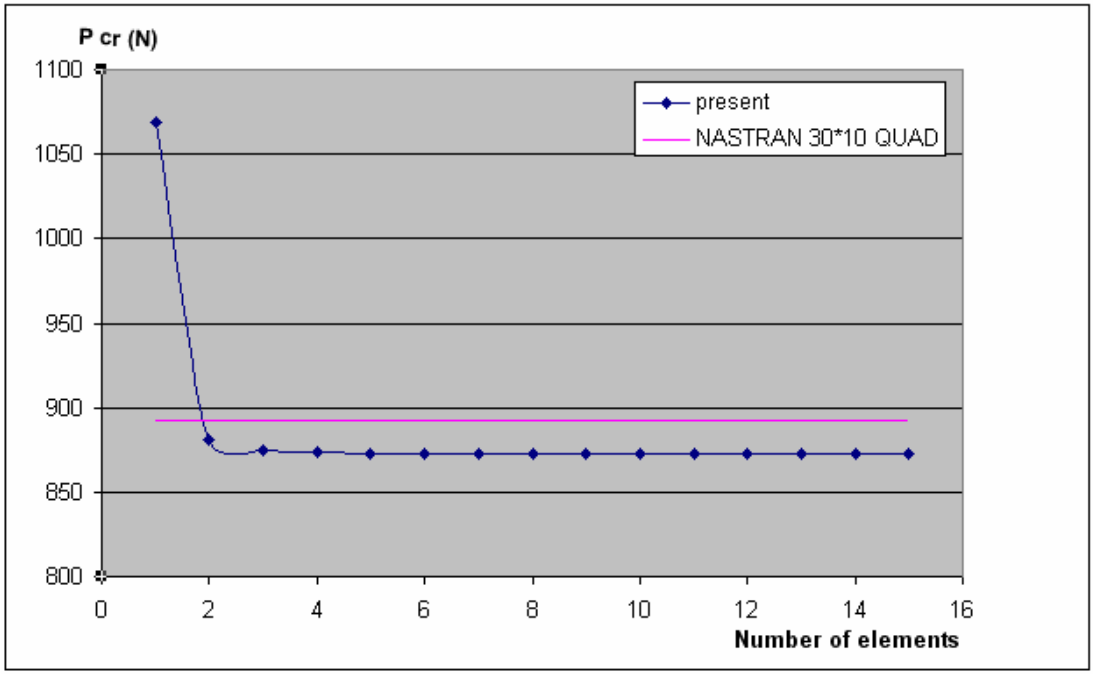

Figure – 5.10 Simply Supported nonuniform rectangular beam buckling loads as a function of number of elements, buckling example 1.

5.7 Buckling of Nonuniform Rectangular Beam - Example 2

In this example, critical buckling loads for nonuniform rectangular Timoshenko beam are examined for various boundary conditions. The results are compared with the results of Auciello & Ercolano's (21) Timoshenko beam Rayleigh - Ritz solution.

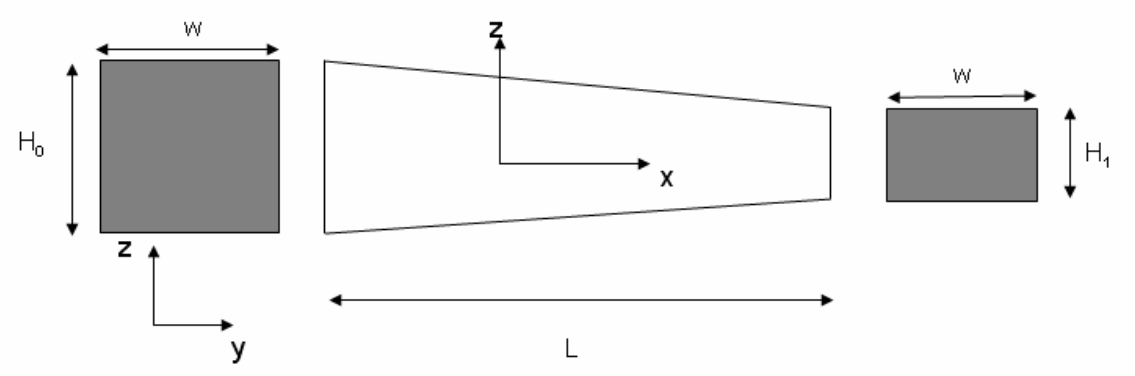

Figure – 5.11 Geometry of nonuniform rectangular beam, buckling example 2

Material and geometric properties are given below:

$E = 210000\,MPa$

$G = 80000\,MPa$

$\nu = 0.3$

$k = 0.833$

$r = \sqrt{\frac{I_0}{A_0}} = 0.1$

Nondimensional critical buckling loads (P_t) of present eight element solution are compared with Auciello & Ercolano's Rayleigh - Ritz solution (21) for various boundary conditions and α values.

Where:

$$P_t = \frac{P_{cr} \cdot L^2}{E \cdot I_0} \quad \text{and} \quad \alpha = \frac{\left(H_1 / H_0 - 1\right)}{L}$$

Table 5.10 –Nondimensional critical buckling loads for nonuniform rectangular beam of example 2.

	Simply Supported - Simplt Supported		Clamped - Free		Clamped - Clamped	
α	Present (N)	Auciello & Ercolano (N)	Present (N)	Auciello & Ercolano (N)	Present (N)	Auciello & Ercolano (N)
-0.4	3.7406	3.9245	1.4395	1.4653	9.7538	10.4961
-0.2	5.3801	5.6787	1.8460	1.8839	13.1081	14.2016
0.1	7.9816	8.5079	2.4321	2.4913	17.8001	19.3318
0.2	8.8649	9.4822	2.6225	2.6898	19.2577	20.9015
0.3	9.7500	10.4645	2.8114	2.8867	20.6514	22.3954
0.4	10.6320	11.4504	2.9981	3.0823	21.9870	23.7648
0.6	12.3752	13.4180	3.3676	3.4691	24.4468	26.2751
0.8	14.0741	15.3584	3.7310	3.8529	26.6208	28.3972
1.0	15.7123	17.2468	4.0894	4.2327	28.4333	30.1126

Figure 5.12 shows present element convergence performance for simply supported beam with $\alpha = 1$.

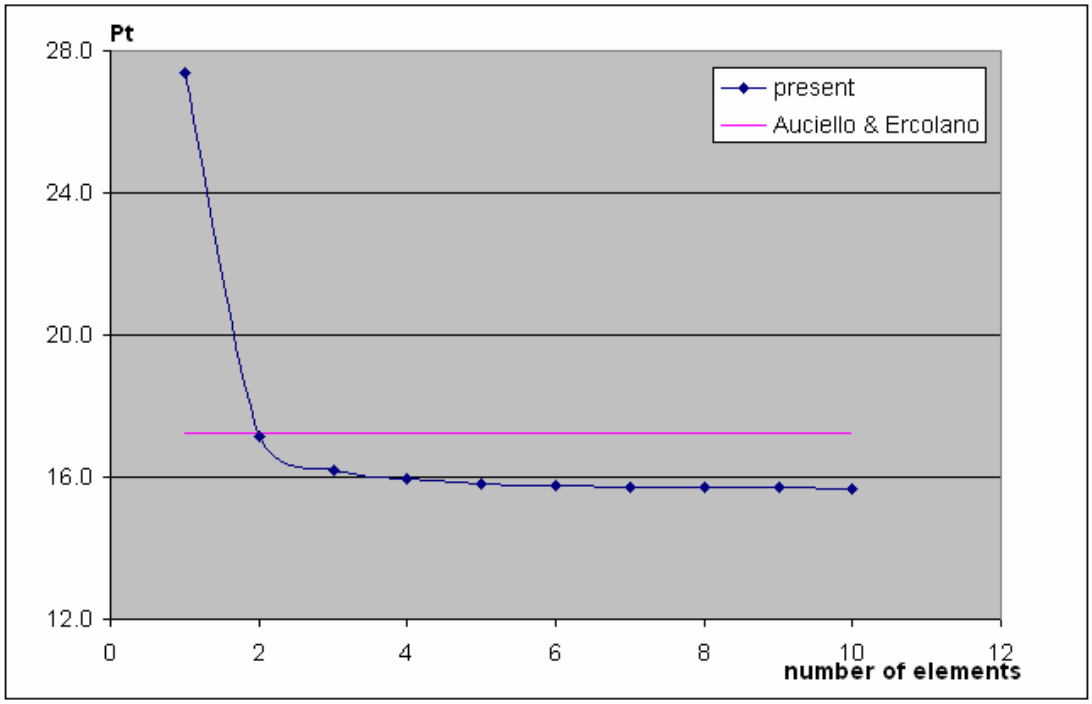

Figure – 5.12 Simply Supported nonuniform rectangular beam buckling loads as a function of number of elements, buckling example 2.

Results of present solution are in good agreement with the Auciello & Ercolano's solutions. From Table 5.9, it can be recognized that relative difference between two solutions can vary with the taper ratio α.

5.8 Buckling of Nonuniform Rectangular Beam - Example 3

In this example, critical buckling loads for nonuniform rectangular Euler – Bernoulli beam are examined.

Geometry and material properties are same as the one in the nonuniform rectangular beam, buckling example 2.

The results of present eight element solution are compared with the results of Rosa & Franciosi's (20) Euler beam exact solution in terms of Bessel functions.

Comparison of nondimensional critical buckling loads (P_t) of present 8 element solution with Rosa and Franciosi's solution for clamped – simply supported boundary and different α values are given in table 5.10.

where

$$\alpha = \frac{H_1}{H_0} - 1 \text{ and } P_t = \frac{P_{cr} \cdot L^2}{E \cdot I_0}$$

Table 5.11 –Nondimensional critical buckling loads for nonuniform rectangular beam of example 3.

α	Present	De Rosa & Franciosi
-0.9	0.8842	0.8748
-0.8	2.1135	2.1189
-0.7	3.6149	3.6344
-0.6	5.3499	5.3884
-0.5	7.2986	7.3622
-0.4	9.4460	9.5434
-0.3	11.7823	11.923
-0.2	14.3017	14.494
-0.1	16.9960	17.252
0.1	22.8868	23.308
0.2	26.0717	26.6
0.3	29.4169	30.063
0.4	32.9113	33.697
0.5	36.5573	37.498
0.6	40.3509	41.465
0.7	44.2859	45.596
0.8	48.3602	49.889
0.9	52.5722	54.343

Figure 5.12 shows present element convergence performance for clamped – simply supported beam with $\alpha = 0.8$.

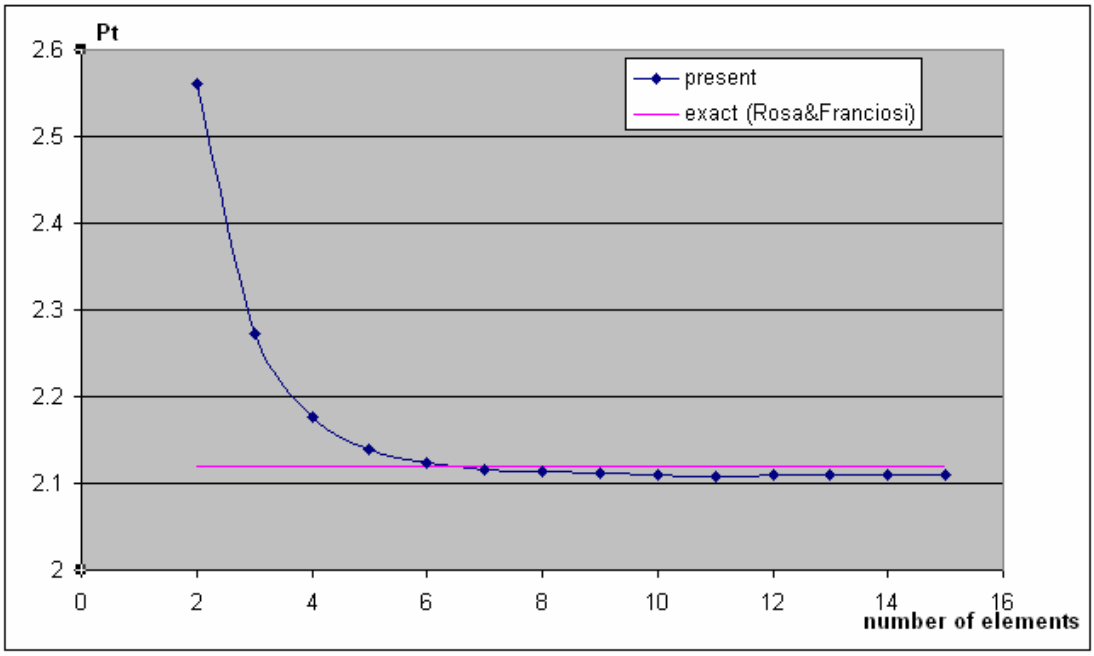

Figure – 5.13 Clamped - Free nonuniform rectangular beam buckling loads as a function of number of elements, buckling example 3.

5.9 Free Vibration of Nonuniform Thin Walled Circular Beam

In this analysis, natural frequencies for nonuniform circular thin walled cantilever Timoshenko beam are investigated for taper ratios, $\beta = 0.6$ *and* 0.8.

where,

$$\beta = \frac{D_1}{D_0}$$

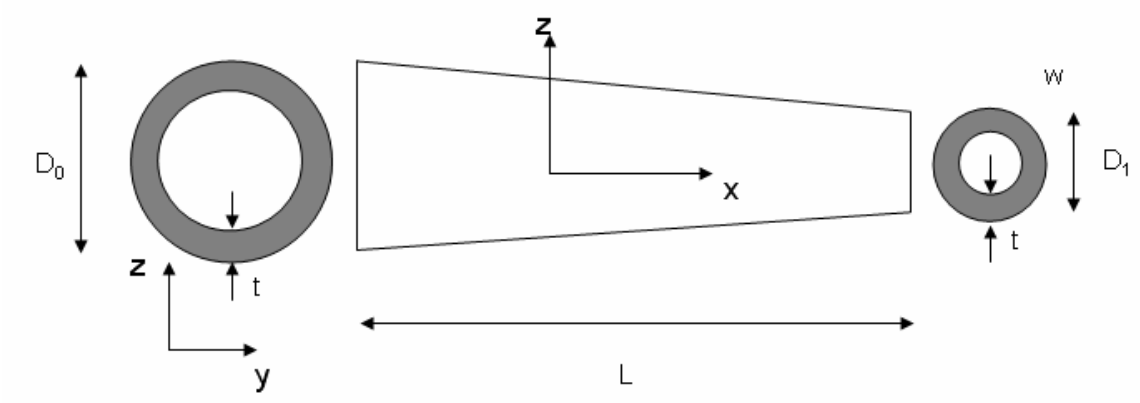

Figure – 5.14 Geometry of nonuniform thin walled circular beam

Material and geometric properties are given below:

$E = 200000\,MPa \quad G = 76923\,MPa \quad \nu = 0.3 \quad k = 0.5 \quad \rho = 7825\ \text{kg/m}^3$

Results with present six element Timoshenko beam solution are compared with To's (17) ten element Timoshenko beam solution in Table 12.

Table 5.12 – Nondimensional natural modes $\left(\sqrt{\frac{\rho A_0}{EI_0}}\cdot\omega\cdot L^2\right)$ of cantilever thin walled circular beam.

	Present (6 element)	To (10 element)
$\beta = 0.6$	3.6713	3.6819
$\beta = 0.8$	3.5297	3.5511

Result of present six element solution is in good agreement with To's ten element solution. Figure 5.15 shows the convergence performance of present element.

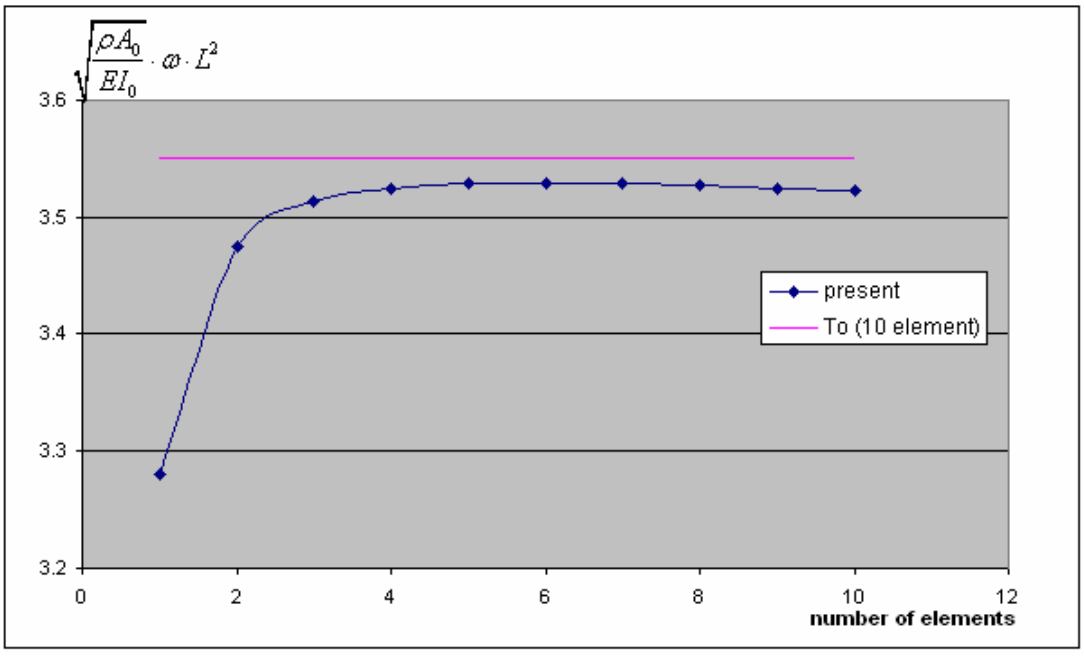

Figure – 5.15 Cantilever nonuniform thin walled circular beam natural modes as a function of number of elements.

5.10 Free Vibration of Nonuniform I - Beam

In this analysis, natural frequency of nonuniform cantilever I-section Euler – Bernoulli beam is analyzed. Beam has constant width, thickness and varying height as shown in Figure 5.12.Result is compared with the Karabalis and Beskos (13) Euler – Bernoulli beam finite element solution.

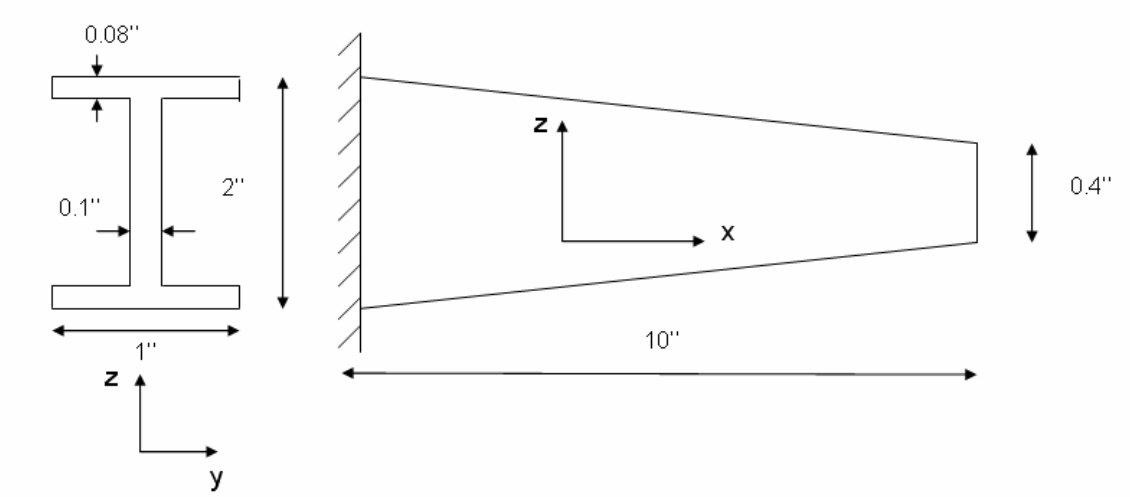

Figure – 5.16 Geometry and boundary conditions of nonuniform I beam, free vibration problem

Material properties are given below:

$E = 1.00\ psi$
$\nu = 0.3$
$\rho = 1.00\, lb \cdot \sec^2 / in^4$

Results obtained by present 20 element yields $w_1 = 0.0257$ *Hertz* .

Karabalis and Beskos 15 element solution gives $w_1 = 0.0262$ *Hertz* .

Present element result is in good agreement with the Karabalis and Beskos's result.

Figure 5.17 shows the present element convergence performance for the free vibration of Euler – Bernoulli I beam problem.

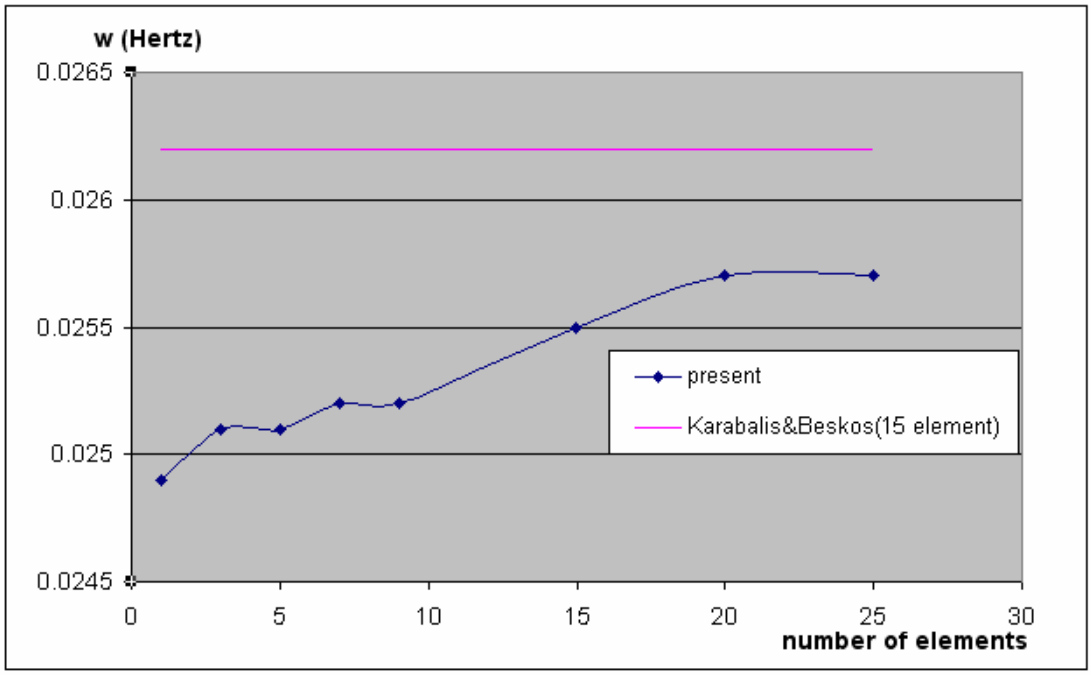

Figure – 5.17 Cantilever nonuniform I beam natural modes as a function of number of elements.

Necessity of high number of elements to convergence is originated from the use of approximate functions in order to express the variation of the cross-sectional properties.

5.11 Buckling of Nonuniform I - Beam

Nonuniform cantilever Euler – Bernoulli I beam problem in Figure 5.18 is solved for critical buckling load. Result is compared with the Karabalis and Beskos (13) Euler – Bernoulli beam finite element solution.

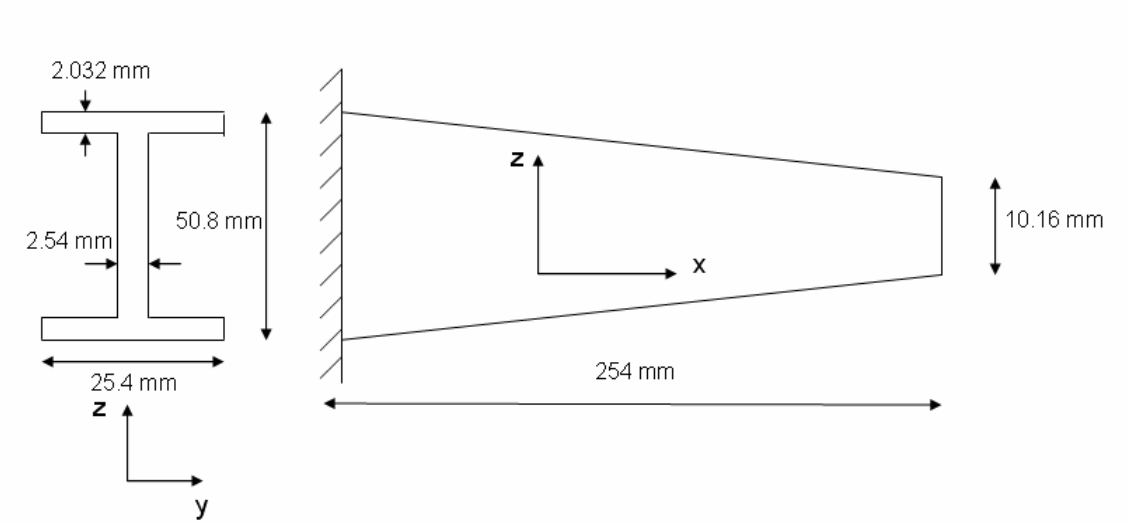

Figure – 5.18 Geometry and boundary conditions of nonuniform I beam, buckling problem

Material properties are given below:

$E = 206850\,MPa$
$G = 80000\ MPa$
$\nu = 0.3$

Results obtained by present 20 element yields $P_{cr} = 243.25\,kN$.

Karabalis and Beskos (13) 5 element solution (13) gives $P_{cr} = 241.08\,kN$.

Present element result is in good agreement with the Karabalis and Beskos's result.

The convergence performance of present element is given in Figure 5.19.

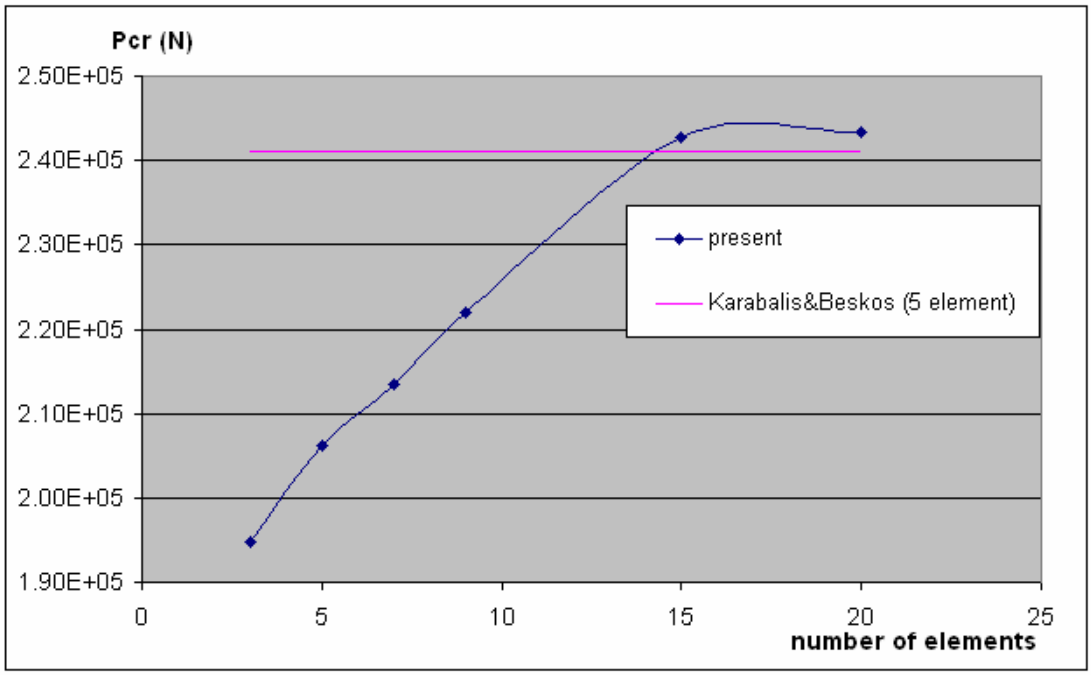

Figure – 5.14 Cantilever nonuniform I beam buckling loads as a function of number of elements.

CHAPTER 6

SUMMARY DISCUSSION & CONCLUSION

This thesis aims to formulate a hybrid finite element for nonuniform Timoshenko beams. For the stability and free vibration analysis, mass and geometric stiffness matrices are also developed.

In the beginning of the study kinematics of deformations are investigated and the displacements are determined in terms of kinematic terms with respect to centroidal axis.

Shear deformations are taken into account via Timoshenko beam theory. Since the study does not concentrated on warping, torsional and distortional warping effects are omitted.

The stress resultants are assumed, so as to satisfy homogeneous equilibrium equations. Boundary tractions are derived in terms of matrix stress resultant coefficients in the matrix form. Then the stiffness matrix is derived from the hybrid stress formulation.

Mass and geometric stiffness matrices are obtained by a new approach which uses the exact displacements through out the beam element. Instead of using assumed displacement fields as in the most of the formulations in the literature, the displacements are obtained directly from homogeneous equations and kinematic

relations. By the use of this method, the mass and geometric stiffness matrices are obtained consistently.

Utilization of exact displacement fields results in better element convergence in stability and dynamic problems.

Formulation of consistent mass and geometric stiffness matrices is a difficult task since the exact displacement functions shall be composed of very complex expressions which includes the variation of cross sectional properties as well as Timoshenko beam constitutive relations.

Derivation of the displacements can be carried out by the help of symbolic manipulation tools (i.e. Mapple 9.5). Even a symbolic manipulation tool may not be sufficient for the beams with complex cross sections such as I beam or thin walled cylinder. In these cases, an approximate representation of the cross sectional properties shall be used, (18). However this method affects the convergence performance of the element depending on how accurate the cross sectional properties are represented with respect to the exact variation of the cross sectional properties.

A finite element solver is prepared using Fortran Power Station to solve the formulation. In this thesis, Gauss elimination method is used with skyline storage technique. Dynamic and stability problems are handled by linear eigenvalue solution with an inverse iteration algorithm.

Present element is assessed by various static, dynamic and stability problems and the results are in good agreement with the results in the literature.

REFERENCES

[1] Tessler, A., and Dong, S. B. "On a Hierarchy of Conforming Timoshenko Beam Elements", Computers and Structures, 14, 335-344, 1981

[2] Tessler, A., and Hughes, T. J. R. "A Three Node Mindlin Plate Element with Improved Transverse Shear", Computing Methods in Applied Mechanical Engineering, 50, 71-100, 1985

[3] Tessler, A., and Hughes, T. J. R. "An Improved Treatment of Transverse Shear in the Mindlin-Type Four Node Quadrilateral Element", Computing Methods in Applied Mechanical Engineering, 39, 311-335, 1983

[4] Pian, T. H. H. "Derivation of Element Stiffness Matrices by Assumed Stress Distributions", AIAA Journal, 2, 1333-1336

[5] Oral, S. "Anisoparametric Interpolation ın Hybrid – Stress Timoshenko Beam Element", Journal of Structural Engineering, 117, 1070-1078, 1991

[6] Newmark, N. M. "Numerical Procedure for Computing Deflections, Moments and Buckling Loads", ASCE, 108, 1161-1188, 1943

[7] Just, D. J. "Plane Frame Works of Tapering Box and I - Section", ASCE, 103, 1977

[8] Lindberg, G. M. "Vibration of Non-uniform Beams", The Aero. Quart., 14, 39-46, 1963

[9] Galagher, G. H., and Lee, C. H. "Matrix Dynamic and Instability Analysis with Non – Uniform Elements", International Journal for Numerical Methods In Engineering, 2, 265 – 275, 1970

[10] Rutledge, W. D., and Beskos, D. E. "Dynamic Analysis of Linearly Tapered Beams", Journal of Sound and Vibration

[11] Timoshenko, S. P., and Gere, J. M. "Theory of Elastic Stability", McGraw Hill, Newyork, 1961

[12] Wang, C. K. "Stability of Rigid Frames with Non-uniform Members", ASCE, 93, 275-294, 1967

[13] Karabalis, D. L., and Beskos, D. E. "Static Dynamic and Stability Analysis of Structures Composed of Tapered Members", Computers and Structures, 16, 731-748, 1983

[14] Lee, S. Y., and Kuo Y. H. "Elastic Stability of Non-Uniform Columns", Journal of Sound and Vibration, 148, 11-24, 1991

[15] Friedman, Z., and, Kosmatka, J. B. "Exact Stiffness Matrix of a Nonuniform Beam – II. Bending of a Timoshenko Beam", Computers and Structures, 49, 545-55, 1993

[16] Romano, F. "Deflection of Timoshenko Beam With Varying Cross-Section", International Journal of Mechanical Sciences, 38, 1017-1035, 1996

[17] To, C. W. S. "A Linearly Tapered Beam Finite Element Incorporating Shear Deformation and Rotatory Inertia for Vibration Analysis", Journal of Sound and Vibration, 78, 475-484, 1981

[18] Gupta, A. K. “Vibration of Tapered Beams”, Journal of Structural Engineering, 111, 19-36, 1985

[19] Cleghorn, W. L., and Tabarrok, B. “Finite Element Formulation of a Tapered Timoshenko Beam for Free Lateral Vibration Analysis”, Journal of Sound and Vibration, 152, 461-470, 1992

[20] De Rosa, M. A., and Franciosi, C. “Higher Order Timoshenko Quotient in the Stability and Dynamic Analysis of Smoothly Tapered Beams”, Journal of Sound and Vibration, 196, 253-262, 1996

[21] Auciello, N. M., and Ercolano, A. “A General Solution for Dynamic Response of Axially Loaded Non-uniform Timoshenko Beams”, International Journal Solids and Structures, 41, 4861-4874, 2004

[22] Rossi, R. E. and Laura, P. A. A. “Numerical Experiments on Vibrating, Linearly Tapered Timoshenko Beams”, Journal of Sound and Vibration, 168 (1), 179-183, 1993

[23] Bathe, J. K. “Finite Element Procedures”, Prentice Hall, 1996

[24] Reddy, J. N. “An Introduction to Finite Element Method”, McGraw - Hill, 2006